

ENGINEERING DESIGN OF OPTIMAL STRATEGIES FOR BLOOD CLOT DISSOLUTION

Scott L. Diamond

*Institute for Medicine and Engineering, Department of Chemical Engineering,
University of Pennsylvania, Philadelphia, Pennsylvania 19104; e-mail:
sld@seas.upenn.edu*

Key Words fibrinolysis, convection, diffusion, plasminogen activator,
myocardial infarction

■ **Abstract** Blood clots form under hemodynamic conditions and can obstruct flow during angina, acute myocardial infarction, stroke, deep vein thrombosis, pulmonary embolism, peripheral thrombosis, or dialysis access graft thrombosis. Therapies to remove these clots through enzymatic and/or mechanical approaches require consideration of the biochemistry and structure of blood clots in conjunction with local transport phenomena. Because blood clots are porous objects exposed to local hemodynamic forces, pressure-driven interstitial permeation often controls drug penetration and the overall lysis rate of an occlusive thrombus. Reaction engineering and transport phenomena provide a framework to relate dosage of a given agent to potential outcomes. The design and testing of thrombolytic agents and the design of therapies must account for (a) the binding, catalytic, and systemic clearance properties of the therapeutic enzyme; (b) the dose and delivery regimen; (c) the biochemical and structural aspects of the thrombotic occlusion; (d) the prevailing hemodynamics and anatomical location of the thrombus; and (e) therapeutic constraints and risks of side effects. These principles also impact the design and analysis of local delivery devices.

CONTENTS

Hemodynamics of Thrombosis	428
<i>Thrombosis Under Flow and In Vivo Thrombi</i>	428
<i>Hemodynamics and Thrombolytic Therapy</i>	430
Blood Clot Biochemistry and Mechanics.....	431
<i>Fibrin Structure and Fibrinolytic Biochemistry</i>	431
<i>Clot Mechanics</i>	432
Biophysics of Thrombolysis.....	434
<i>Diffusion</i>	434
<i>Dispersion</i>	435
<i>Permeability</i>	435
<i>Adsorption Phenomena</i>	437

Reaction Engineering Analysis	437
<i>Mathematics of Fibrinolysis</i>	437
<i>Assay Methods and Boundary Conditions</i>	442
<i>Diffusion-Mediated Lysis</i>	443
<i>Permeation-Enhanced Lysis</i>	444
Intravenous Lytic Therapies	446
<i>Pharmacokinetics</i>	446
<i>Pharmacodynamics</i>	446
Catheter-Based Therapy	449
Designing Lytic Formulations	452
Clot Cannulation	453
Summary	453

HEMODYNAMICS OF THROMBOSIS

Thrombosis Under Flow and In Vivo Thrombi

The development of a thrombus, its structure, and its susceptibility to lysis depend on complex interactions of biology and hydrodynamics. The coagulation cascade triggered by the exposure of tissue factor within the ruptured atherosclerotic plaque results in conversion of prothrombin to thrombin. Thrombin cleaves fibrinopeptides A and B from fibrinogen resulting in a fibrin monomer that undergoes polymerization. The capture of flowing platelets by exposed subendothelium involves platelet GP Ib–von Willebrand factor (vWF) interactions followed by slower but more stable fibrinogen cross-bridging of platelet GPIIb/IIIa ($\alpha_{IIb}\beta_3$) (97, 124). Neutrophils and monocytes can also be captured into platelet thrombi via platelet P-selectin to further enhance fibrin deposition (78).

Arterial flow conditions with high wall shear rates increase platelet deposition and decrease red blood cells (RBCs) and fibrin accumulation, whereas low shear rates are more permissive for fibrin formation and retention of RBCs (125). Clots formed under flow in vivo or in Chandler loops display marked striations indicative of an ongoing deposition-mediated growth. Such clots have upstream “head” regions rich in platelets, leukocytes, platelet-released plasminogen activator inhibitor type 1 (PAI-1), and downstream “tail” regions enriched in RBCs (89, 106). Coronary artery thrombi formed during unstable angina are grayish white, whereas those present during acute myocardial infarction (MI) are reddish in appearance as determined by angioscopy (69). These grayish-white coronary thrombi tend to be resistant to thrombolytic therapy. These structures are particularly rich in platelets, are older, have a very tight fibrin structure (113), and are formed under flow conditions. The reddish thrombi of acute MI are fibrin and RBC rich and tend to be younger.

Once formed, blood clots are defined by two interpenetrating pharmacological compartments: (a) the impermeable cellular compartment that contains platelets, RBC, and white blood cells, and (b) the permeable biphasic fibrin gel compart-

ment that contains hydrated fibrin fibers surrounded by fluid. The biphasic fibrin gel has a porosity $\varepsilon = V_{\text{void}}/V_{\text{total}}$, which may vary with position in the clot. During thrombolysis, the fibrinolytic reactions occur in the biphasic fibrin to erode the solid phase volume of the fibrin fibers ($\phi = 1 - \varepsilon$). Average concentrations of reactive species within the fibrin gel can be defined based on their local phase-averaged concentration within the fibrin fiber volume or the pore space volume.

Venous and arterial thrombi compositions have been measured *ex vivo* (82), and these levels are given in Table 1. Because thrombi form under flow conditions, the relationship of clot properties to those of whole blood is not a direct one; depletions and enrichments occur (15, 19, 82). Also, a real thrombus experiences compacting forces and the permeation of fresh fibrinogen that would allow for continuing fibrin polymerization.

TABLE 1 Initial state of systemic circulation and arterial and venous thrombi

Species	Plasma (μM)	α -Granule release (μM) ^a	Thrombi level (μM) ^b	
			Venous	Arterial
Fibrin(ogen)	8.0	0.044	$c_T = 80\text{--}220$	
Plasminogen	2.2	0.00136	$c_i = 0.562$ $s_i = 1.299$ $c_T = 0.783$	$c_i = 0.839$ $s_i = 2.428$ $c_T = 1.316$
tPA ^c	0.00005	— ^d	$c_i = 0.000618$ $s_i = 0.00133$ $c_T = 0.000832$	$c_i = 0.000917$ $s_i = 0.00309$ $c_T = 0.00157$
uPA ^e	0.00005	—	$c_i = 0.00005$ $s_i = 0$ $c_T = 0.000035$	$c_i = 0.00005$ $s_i = 0$ $c_T = 0.000035$
Plasmin	0	—	—	—
PAI-1 (only 5% active)	0.0003	0.00447	$c_i = 0.0274$ $s_i = 0.0071$ $c_T = 0.0213$	$c_i = 0.0617$ $s_i = 0.00858$ $c_T = 0.0458$
α_2 -Antiplasmin	1.0	0.000269	$c_i = 1.0$ $s_i = 1.0$ $c_T = 1.0$	$c_i = 1.0$ $s_i = 1.0$ $c_T = 1.0$
Macroglobulin	3.0	0.00171	$c_i = 3.0$ $s_i = 0$ $c_T = 2.1$	$c_i = 3.0$ $s_i = 0$ $c_T = 2.1$
Platelets	$0.3 \times 10^9/\text{ml}$	—	$1.5 \times 10^9/\text{ml}$	$4.5 \times 10^9/\text{ml}$

^aBased on release of α -granules from 0.3×10^9 platelets into 1 ml of buffer.

^bDerived from Potter van Loon et al (82). For porosity, $\varepsilon = 0.7$ corresponding to 0.3 g of pellet/g of thrombi, the total clot concentration of each species ($c_T, \mu\text{M}$) is given as $c_T = \varepsilon c_i + (1 - \varepsilon)s_i = [\mu\text{g of free/g of thrombi} + \mu\text{g of bound/g of thrombi}]/(1000/\text{MW})$.

^ctPA, Tissue plasminogen activator.

^d—, Negligible.

^euPA, Urokinase.

Hemodynamics and Thrombolytic Therapy

Clinical evidence indicates an important role for permeation and its impact on the rate at which reperfusion occurs. For example, patients with hypotension or cardiogenic shock are poor candidates for successful thrombolytic treatment of myocardial infarction (38, 83). In human cardiogenic shock and MI, the success of thrombolytic therapy can be enhanced with administration of inotropic agents (with a consequent increase of systolic pressure from 64 to 102 mm Hg) (38). In a canine model of left anterior descending coronary thrombosis with severe hypotension (systolic pressure of 75 mm Hg) (85), left anterior descending catheter administration of recombinant tissue plasminogen activator (tPA) to the clot was significantly less effective under conditions of hypotension when compared with thrombolysis at systolic pressures of 130 mm Hg. Similar transport mechanisms have been shown for the lysis of pulmonary embolism (84, 88). In a canine model of cardiogenic shock with left anterior descending thrombosis in which systolic pressure had been reduced to 75 mm Hg by phlebotomy, intraaortic balloon counter pulsation to increase coronary pressure resulted in enhanced thrombolysis, with intravenous (i.v.) tPA (86, 87). The transport issues in various clinical trials have been reviewed by Blinc & Francis (9).

MI is a thrombotic event triggered by atherosclerotic plaque rupture. The upstream pressure on a clot is the time-averaged aortic pressure of ~ 90 mm Hg, whereas the downstream pressure depends on the extent of collateralization of the myocardium. Collateralization is known to reduce infarct size during MI due to reduction of ischemia (28, 80). There is a report of thrombolysis being less successful in patients with collateralization, but this was correlated with enhanced severity of stenosis in this patient subset (4). For a 1-cm-long clot (68), the pressure drop ($\Delta P/L$) across an occlusive arterial thrombus may range from ~ 70 – 80 mm Hg/cm to ~ 40 mm Hg/cm with collateralization.

In stroke, occlusion occurs as a result of (a) local atherothrombosis of a large or small cerebral vessel or (b) through embolization from a noncerebral source such as an atherothrombotic carotid artery or the fibrillating heart. Cerebral and subarachnoid hemorrhages, for example caused by aneurysm rupture, are distinct causes of stroke and highly contraindicated for thrombolytic therapy. Thrombotic stroke can occlude the basilar, vertebral, or carotid arteries. Embolic material from the carotid or atria has not been quantified for differences in fibrin density or lytic susceptibility. A clot that occludes the vertebral, basilar, or carotid arteries can experience a mean arterial pressure of ~ 75 mm Hg with $\pm 20\%$ pulsatility on its proximal face. It is difficult to estimate the pressure on the distal face of the clot, which may at times approach the proximal pressure due to the complex connectivity of the cerebral circulation. The role of collateral blood flow was found to provide no benefit for thrombolysis of proximal basilar thrombosis but reduces ischemia in basilar artery thrombolysis (30).

In deep vein thrombosis, clots are formed under low flow conditions or stasis, often after surgery, by mechanisms likely involving inflammatory pathways and

venous dysfunction. These clots are RBC rich and are extremely long, with lengths from a few centimeters to ~ 25 cm. The pressure drop across these long clots is low (< 1 mm/cm of clot). Thus, deep vein thrombosis is not susceptible to i.v. therapy due to poor drug penetration. Thrombolytic therapy requires intrathrombic delivery via catheters that are continually pushed through the deep vein thrombosis over several hours to days. Similarly, in peripheral arterial thrombosis, the 5- to 25-cm-long clots (47) experience pressure drops of ~ 5 – 10 mm Hg/cm, insufficient to drive substantial permeation.

In pulmonary embolism, in which an embolus from a deep vein thrombosis lodges in the pulmonary arterial circulation to obstruct flow, the local pressure drop across the embolism can be estimated by using the mean pulmonary artery pressure of about 20 mm Hg as the upstream pressure and the mean left atrium pressure to estimate the pulmonary venous pressure. For a 1-cm-long pulmonary embolism, the mean pressure drop $\Delta P/L$ is 10 mm Hg/cm of clot (7–15 mm Hg/cm over the cardiac cycle). The pulmonary embolism would have a permeability similar to a retracted whole blood clot subjected to arterial compacting forces ($k \sim 10^{-10}$ – 10^{-12} cm²), thus providing a Darcy flow velocity of ~ 0.05 mm/min.

In arteriovenous access grafts for dialysis patients, a large ΔP exists (40–80 mm Hg) across clots that may be several centimeters long. The ease of access to the graft facilitates local infusions. Urokinase (uPA) has a higher probability of deep penetration because it does not bind fibrin and is more commonly used to clear access grafts.

BLOOD CLOT BIOCHEMISTRY AND MECHANICS

Fibrin Structure and Fibrinolytic Biochemistry

The thrombin-activated fibrin monomers polymerize into extended protofibrils (2 monomers thick) that aggregate laterally to form thick fibers (for review, see 42). Structural and transport properties of fibrin are given in Table 2. Ionic strength was long held to regulate electrostatic interactions during protofibril lateral aggregation, but recent evidence has implicated the prevailing chloride ion as a fibrin-binding inhibitor of lateral aggregation leading to extremely thin fibers in the fibrin gel (32). Thin fiber gels of fibrin are noted to dissolve more slowly (37). Coarse clots with thick fibers formed from plasma at lower ionic strengths and low thrombin or in the presence of dextran dissolved more rapidly than fibrin clot structures when treated with tPA or uPA (23).

Fibrinolysis is a multicomponent and multiphase reaction network (Figure 1). uPA can activate plasminogen to plasmin in a homogeneous fluid phase reaction, whereas tPA can bind fibrin and activate fibrin-bound plasminogen in a heterogeneous reaction. PAI-1 and α_2 -antiplasmin inhibit plasminogen activators (uPA and tPA) and plasmin, respectively. As fibrin is cleaved by plasmin, new binding sites for plasminogen, plasmin, and tPA are revealed with the generation of car-

TABLE 2 Structural and transport properties of fibrin and blood clots

Property	Measurement
Fibrinogen, 340 kD	45 nm × 2 nm
r_o , Radius of hydrated photofibril	3–5 nm (2 monomers/fibril)
Radius of fundamental fiber unit	50 nm
R_f , Radius of hydrated fiber bundle	4–50 nm (Fine gel at 0.3 M NaCl) 100–500 nm (Coarse gel at 0.1 M NaCl)
Pores between protofibrils in fiber	10–30 nm
D_{pore} , Diameter of pore in fibrin gel	0.1 (fine) to 10 μ M (coarse)
Fibril density in fiber	0.01116 Fibrils/nm ² (coarse) 0.008366 Fibrils/nm ² (fine)
Fiber porosity	0.80 (coarse)
Fiber density	210 mg/ml of fiber (fine) 280 mg/ml of fiber (coarse)
ϵ , Overall porosity	>0.99 (Plasma or purified fibrin gel) 0.9 – 0.99 (Platelet-retracted clots) 0.75 – 0.9 (Compacted fibrin)
k , Specific permeability	10 ⁻⁸ cm ² (Coarse fibrin, 3 mg/ml) 10 ⁻¹⁰ – 10 ⁻¹¹ cm ² (Fine fibrin, 3 mg/ml) 10 ⁻⁸ cm ² (Unretracted whole blood or plasma clot) 10 ⁻¹⁰ cm ² (Retracted whole blood) 10 ⁻¹¹ – 10 ⁻¹³ cm ² (Compacted coronary thrombus)
Reynolds number, $Re = \rho L v/\mu$	0.1 – 1 Global ($\rho L_{clot} v/\mu$) $Re \ll 0.001$ Local ($\rho D_{fiber} v/\mu$)
Peclet number, $Pe = vL/D_L$	$O(10^3)$ Global $O(1-100)$ Local at lysis front
$\Delta P/L$	~60 mm Hg per cm of clot (arterial) 0–10 mm Hg per cm of clot (venous)

boxy-terminal lysines (44). These lysines can be subsequently removed by thrombin-activated carboxypeptidases in plasma (123).

Clot Mechanics

The rheology of purified fibrin, platelet-free plasma, or platelet-rich plasma clots is accurately described by linear viscoelastic theory for small deformations, in which the complex dynamic shear modulus G is defined as $G = G' + iG''$, where G' [=] dyne/cm² is the dynamic elastic modulus (which scales with the cross-link density) and G'' is the dynamic loss modulus (which describes viscous flow behavior and is much smaller than G'). The elastic modulus G' can increase with strain, i.e. strain hardening (5). Glover et al (39) provide a correlation for the maximum elastic modulus obtained after complete platelet-rich-plasma clotting post-recalcification as $G'_{max} = 420 + 0.54 p^{0.76}$ for p = platelet concentration

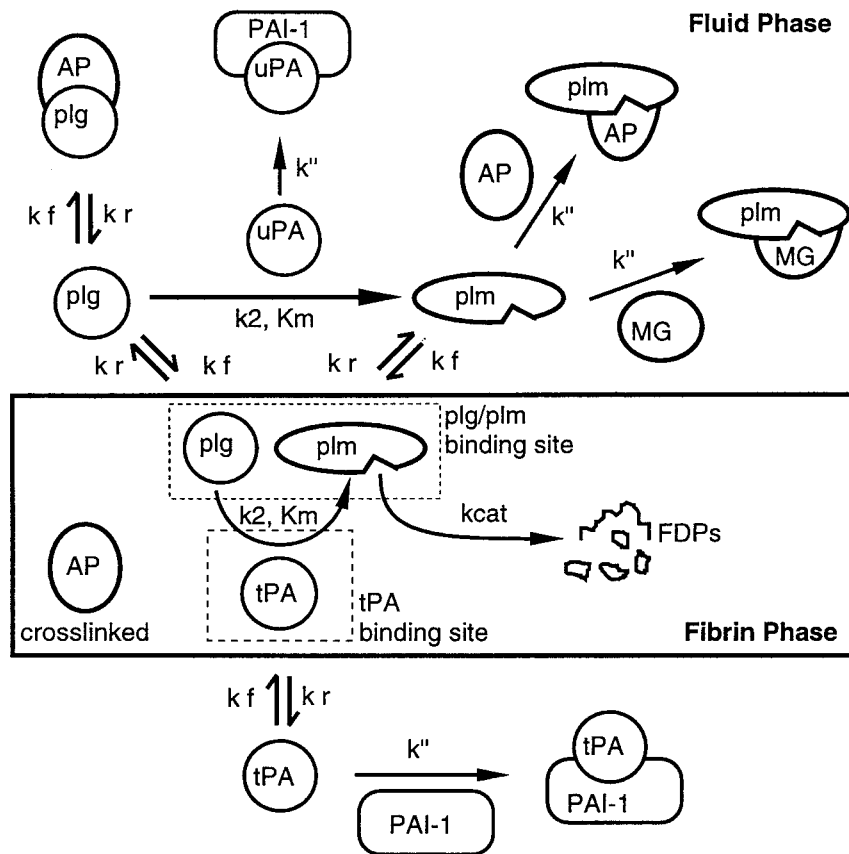


FIGURE 1 Schematic of fibrinolysis. Plasminogen (plg) is activated to plasmin (plm) in the fluid phase by urokinase (uPA), whereas fibrin-bound plasminogen is activated by tissue plasminogen activator (tPA) in the fibrin phase. The free-phase plasmin is inhibited by the antiplasmin (AP) and macroglobulin (MG), whereas the bound-phase plasmin is protected from inhibition. The uPA and tPA are inhibited in the free phase by plasminogen activator inhibitor type 1 (PAI-1). Plasmin solubilizes fibrin to fibrin degradation products (FDP). Soluble species can reversibly adsorb and desorb with fibrin under kinetically controlled conditions.

(platelets/mm³), where platelets significantly enhance clot strength. The value of G'_{max} is ~ 1000 dyne/cm² for clotted platelet-free plasma or platelet-poor plasma, ~ 3000 dyne/cm² for clotted whole blood, and $\sim 10,000$ dyne/cm² for clotted platelet-rich plasma. Platelet retraction can generate significant normal forces (60), and retracted clots are well known to display lytic resistance through mechanisms involving PAI-1 (17). The relationship between evolving clot mechanics during lysis and embolization has not been well characterized experimentally. For

flow around a nonoccluding wall-attached thrombus, the shearing and normal forces on the surface that cause embolization are not affected by pressure-driven permeation through the thrombus (6). However, such permeation would control delivery of plasminogen activators.

BIOPHYSICS OF THROMBOLYSIS

Diffusion

The penetration of proteins entering a fibrin clot as well as their mobility within the fibrin gel represents a complex transport problem. In general, the Brownian motion of a protein in fibrin would experience minimal steric hindrance or hydrodynamic resistance because the ratio λ of the protein radius (4 nm) to the typical pore radius (>500 nm) is quite small ($\lambda < 0.01$). For a random array of fibers of radius R_f and fiber volume fraction ($\phi = 1 - \epsilon$), the pore-averaged diffusivity \bar{D} of a solute with radius R_s is given by Ogston et al (77) as $\bar{D}/D_o = \exp(-\phi^{1/2} R_s/R_f)$, which accounts for steric hindrance but not hydrodynamic resistance. The Brownian diffusion coefficient of numerous proteins in water (D_o) is correlated by Tyn & Guzek (112) with $D_o \sim 5 \times 10^{-7}$ cm²/s being typical for most mid-sized proteins. For a coarse fibrin gel at 8 μ M, the ratio is $\bar{D}/D_o > 0.99$ for a protein with 4 nm radius and a fiber with a 250 nm radius. For a compacted fibrin gel (at 220 μ M, $\phi \sim 0.3$), the ratio remains >0.99 . Hindered Brownian diffusion of a spherical solute in a cylindrical pore (18, 75) that accounts for hydrodynamic resistance $\{\bar{D}/D_o = [1 - \lambda]^{-2}[1 + (9/8)\lambda \ln \lambda + 1.539\lambda + 1.2\lambda^{-2}]\}$ indicates minimal hindrance of solute mobility in plasma gels. Consideration of hindered Brownian diffusion of a spherical solute in a fiber matrix with hydrodynamic interactions (81), in which $\bar{D}/D_o = [(1 + (R_s^2/k)^{1/2} + 1/3(R_s^2/k))^{-1}]^{-1}$, indicates that hindrance of solute mobility is minor (<10% reduction in mobility) for fibrin with a Darcy permeability $k > 10^{-11}$ cm² (a retracted clot). Hindrance is more substantial ($\bar{D}/D_o \sim 0.4$) in a highly compacted clot when the Darcy permeability is estimated to be $\sim 10^{-13}$.

These calculations are consistent with the lack of reduction of the diffusivity of proteins in 30% retracted whole blood clots (66). Also, fluorescent bovine serum albumin displays only modest 40% reduction in diffusivity at 12 mg/ml of fibrin (105); however, the albumin was present during fibrinogen polymerization in this measurement. Sakharov et al (93) measured the penetration of fluorescent antifibrin(ogen) from a creeping flow into a plasma clot. Strong fibrin binding of the antibody resulted in a <200- μ m penetration in 1 h, whereas a nonimmune antibody penetrated >500 μ m into the plasma clot, consistent with unhindered Brownian diffusion. Steric and hydrodynamic resistance become important in understanding mobility of a protein within the 10- to 30-nm spaces between the protofibrils of the fibrin fiber (8, 25, 119).

Dispersion

Dispersion represents the sum of molecular diffusion and convection-enhanced mixing across fluid streamlines (92). A common form of the longitudinal dispersion coefficient D_L for inert solutes is given as the sum of the effective diffusion coefficient and hydrodynamic dispersion. The effects of adsorption and reaction on D_L are not known, although these processes may reduce the amount of solute in the slowest moving streamlines near the solid fiber surface (99) so as to enhance dispersion.

Dispersion, even when fluid permeation is present, has an important role in fibrinolysis. In finite-thickness, moving-front systems, dispersion dictates the shape of species peaks at the lytic front (114) where sharp gradients can exist and where the local Peclet number, Pe_{local} , is actually small. The $Pe_{local} = v_{front} \delta_{front}/D_L$ is about 2–20, for a front velocity (v_{front}) of $0.1 \times$ the Darcy velocity (\bar{v}) to $1.0 \times \bar{v}$, a lysis front thickness of $\delta_{front} \sim O(100 \mu\text{m})$, and the longitudinal dispersion D_L scaling with $D_{pore} \bar{v}$. The Pe_{local} is significantly smaller than the global Peclet number $Pe = (\bar{v} \cdot L_{clot})/(D_{pore} \bar{v}) \sim O(1000)$. Neglect of dispersion at the lysis front is not justified by the magnitude of Pe_{local} , and such neglect will overestimate the height of the species at the front, where large gradients exist over small length scales.

Permeability

The permeability of a fibrous structure is dictated by the porosity and fiber diameter. Fine fiber gels offer considerably higher resistance to pressure-driven permeation when compared with coarse fiber gels formed at the same fibrin concentration. Permeability measurements of fibrin were first conducted as a probe of molecular structure to estimate pore size and fiber thickness. Permeability of $\sim 10^{-10} \text{ cm}^2$ for 9.4-mg/ml of fibrin led to estimates of 30- to 70-nm fiber diameters (90). At 2 mg/ml, fine gels have a permeability of $4 \times 10^{-11} \text{ cm}^2$, and coarse fibrin has a permeability of $4 \times 10^{-9} \text{ cm}^2$ (25). Recalcified, thrombin-treated human plasma (undiluted) has a permeability of 1×10^{-8} to $4 \times 10^{-8} \text{ cm}^2$, depending on the speed of coagulation (13). Polymerization of plasma can produce very thick fibers (22). The presence of RBCs during polymerization of whole blood (diluted by half in buffer) results in very large pores that allow the elution of RBCs, suggesting a pore size similar to that of the deformable RBC (24). The permeability of clotted plasma was found to be slightly lower in patients with a history of MI, compared with an age-matched control group ($8.3 \pm 5.2 \times 10^{-9} \text{ cm}^2$ vs $12.5 \pm 5.7 \times 10^{-9} \text{ cm}^2$) (35). Fibrinogen levels can be 1.5- to 3-fold higher in patients with a history of MI. Interestingly, low-dose acetylsalicylic acid (75 mg daily dose) taken by a healthy control group increased plasma clot permeability by 65%, and this increase reversed 1 week after stopping the dosage (127).

Correlations become useful to predict the permeability of a structure of known fibrin density and fiber radius. Correlations for random arrays of cylinders average the contributions of parallel and perpendicular orientations (48). For aligned cylinders, flow perpendicular to the cylinders results in only a twofold increase in resistance relative to flow parallel to the cylinders. Thus, the anisotropic nature of the fiber orientation and permeability compared with flow direction is not unusually strong and may be offset by the observation that spatial nonuniformity can increase the permeability by $\leq 50\%$ (48). The correlation of Jackson & James (48) of $k = D_{\text{fiber}}^2 (3/80 \phi) (-\ln \phi - 0.931)$ is applicable to numerous fibrous media, but tends to underpredict the permeability for highly porous gels (50) as well as for fibrin gels. Diamond & Anand (31) found that the specific permeability data of Blomback et al (14) were suitably correlated with the fiber diameter and the fibrin porosity by the Davies equation (33), where

$$k = D_{\text{fiber}}^2 / [70(1 - \varepsilon)^{3/2} \{1 + 52(1 - \varepsilon)^{3/2}\}] \quad (1)$$

The permeability of a platelet-retracted, whole blood clot can be estimated from correlations for fibrin permeability $k(\varepsilon_{\text{rf}}, D_{\text{fiber}})$, where ε_{rf} is the porosity of the retracted fibrin that resides in the volume between the RBCs. A whole blood clot cannot retract more than $\sim 50\%$, because the RBCs are incompressible. Clotted blood initially having a hematocrit $H = 0.35\text{--}0.5$ can undergo a global retraction R^G (e.g. $R^G = 0$ for no retraction to $R^G = 0.5$ for 50% retraction to 0.5 of original volume). By considering the volume of each compartment in a retracted clot and the volume of exuded serum, it is possible to define C , the compaction of the fibrin within the volume surrounding the RBCs as

$$C = [R^G - (H + (1 - H)\alpha)] / [(1 - H)(1 - \alpha)] \quad (2)$$

where $\alpha = \rho_{\text{fibrinogen in plasma}} / \rho_{\text{fibrinogen in fibrin fiber}} = 0.0171$ (coarse fiber) to 0.0143 (fine fiber).

The overall permeability of the retracted clot $k_{\text{retracted clot}}$ is then given as

$$k_{\text{retracted clot}} = k(\varepsilon_{\text{rf}}, D_{\text{fiber}}) \cdot [(1 - H)\alpha + C(1 - H)(1 - \alpha)] / [H + (1 - H)\alpha + C(1 - H)(1 - \alpha)], \quad (3)$$

where $\varepsilon_{\text{rf}} = [C(1 - \alpha)] / [\alpha + C(1 - \alpha)]$.

For a 50% retraction of clotted whole blood ($R^G = 0.5$, $H = 0.4$), the clotted plasma in the clot will have been compacted to 15.8% of its original volume ($C = 0.158$), corresponding to an exudation of 84.2% of the original plasma volume as serum from the retracted clot. Under these conditions for $\varepsilon_{\text{rf}} = 0.93565$ and the plasma coarse fiber diameter $D_f = 380$ nm (22), the permeability of the 55.8- μM fibrin in the volume between the RBCs is given by Eq. 1 as 0.5×10^{-9} cm^2 . The value of $k_{\text{retracted clot}}$ is then calculated to be 1.0×10^{-10} cm^2 , which compares well with the single measurement in the literature of 1.13×10^{-10} cm^2 (134). It is reasonable to conclude that the transport property of the fibrin within a retracted clot is largely determined by the permeability of dense fibrin. Similarly, for clotted

whole blood that is not retracted ($R^G = 0$, $H = 0.4$, $C = 1.0$, $\alpha = 0.0171$), the overall clot permeability is estimated to be $0.9 \times 10^{-8} \text{ cm}^2$ (380-nm fiber diameter), which compares reasonably well with the measurement of $1.22 \times 10^{-8} \text{ cm}^2$ (12) for undiluted clotted whole blood without retraction.

Adsorption Phenomena

Although forward binding events may equilibrate rapidly relative to the time scale of thrombolysis and transport, dissociation events are considerably slower. Bound proteins may coexist with fluid depleted of the protein due to washout by permeation. This represents a nonequilibrium state. Additionally, there exist numerical difficulties that prevent the application of the local equilibrium assumption. In moving-front problems with finite thickness, the solubilization at the lytic front is a spatially dependent source term. In any numerical solution involving discretization, two adjacent elements are coupled by convection, which links soluble-phase species in the upstream element (released by lysis) with the fluid concentration at the downstream node. Thus, solubilization is a source term in the upstream element that erroneously forces the phantom creation of mass in the solid fibrin in the downstream element when local equilibrium is enforced.

Dissociation constants (K_d) of fibrinolytic species binding with fibrin are available. The adsorption and desorption rates of proteins interacting with fibrin have not been measured, partly because fibrin is an insoluble polymer that is difficult to handle in stop-flow or surface plasmon resonance measurements. The forward association rates for proteins binding to fibrin are expected to be significantly less than the ultrafast and very high-affinity associations of plasmin with antiplasmin ($k_f = 10^7 \text{ M}^{-1} \text{ s}^{-1}$) (128), plasmin with α_2 -macroglobulin ($k_f = 0.03 \times 10^7 \text{ M}^{-1} \text{ s}^{-1}$) (118), and tPA binding with PAI-1 ($k_f = 2.9 \times 10^7 \text{ M}^{-1} \text{ s}^{-1}$) (62). Protein forward-association rates have often been measured by surface plasmon resonance to be $\sim 10^3$ – $10^6 \text{ M}^{-1} \text{ s}^{-1}$, often slower than diffusion-limited association. A time of 10 min was clearly sufficient for equilibration of protein binding to fibrin (64). Because the binding of fibrinolytic mediators to fibrin is a fast process (likely equilibrating within seconds) relative to the characteristic times of lysis kinetics and front propagation, modeling of fibrinolysis may not be highly sensitive to the value for the forward adsorption rate, except in situations in which a reactive species is generated in solution and a competition exists between its rate of adsorption and its rate of inhibition.

REACTION ENGINEERING ANALYSIS

Mathematics of Fibrinolysis

The mathematics describing moving fronts in dissolving permeable media including polymers are well established (34, 76, 79). Fibrinolysis is a multicomponent reaction network with fluid-phase reactions as well as heterogeneous reactions

catalyzed by species bound in the solid-fibrin fiber phase. The analogy with affinity chromatography is particularly useful, except that the solid phase can disappear, which results in solubilization and rebinding of species (Figure 2A). In this case, the moving lysis front operates like an "affinity filter," whereby species accumulate at the front based on their binding affinity to fibrin. For transport of species in eroding fibrin, the instantaneous concentration of a soluble species at some position in the fluid phase of the fibrin gel is described by Eq. 4-6 (1-3; see also 7, 55, 76, 79, 126).

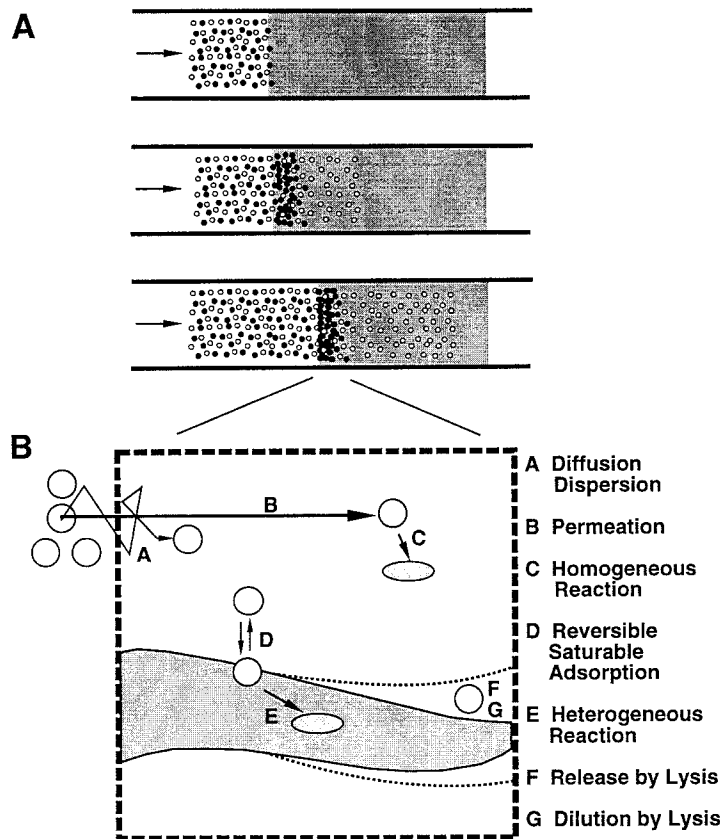


FIGURE 2 Summary of transport and reaction physics during fibrinolysis. (A) Solutes that do not bind fibrin permeate with the solvent front, whereas fibrin-binding species accumulate at the lysis front as fluid permeates into the fibrin where they undergo continual solubilization and rebinding. (B) At each position of the clot, various physical and biochemical processes affect the concentration of species in the fluid and fibrin phases as well as the volume of each phase.

The rate of change of the local volume-averaged concentration of the i th species in the fluid phase (c_i) depends on the net transfer rate of that species to the fibrin fibers ($\partial N_i^T/\partial t$), dispersion (D), permeation (v), homogeneous reaction in the free phase between the l and k species (R_{lk}), and the effects due to change of volume of the solid phase ($\partial \varepsilon/\partial t$) as adsorbed species (s_i) are released during solubilization of the solid phase and free phase species are diluted to a small extent in the lost fibrin fiber volume (Figure 2B). The rate of change of a fibrin-bound concentration of the i th species depends on the heterogeneous rate of reaction in the solid phase ($^sR_{lk}$), the rate of binding, and the rate of dissociation under conditions where the j th species may compete for the r th binding site (for $\xi_{rj} = 1$, interaction; for $\xi_{rj} = 0$, no interaction) (see Eq. 5).

$$\varepsilon \frac{\partial c_i}{\partial t} = (s_i - c_i) \frac{\partial \varepsilon}{\partial t} - (1 - \varepsilon) \frac{\partial N_i^T}{\partial t} + \nabla \cdot (D \cdot \nabla (\varepsilon c_i)) - \nabla \cdot (\varepsilon c_i v) + \varepsilon \sum_l \sum_k R_{lk}^i. \quad (4)$$

$$\frac{\partial N_i^T}{\partial t} = k_{r,i}^r c_i (\theta_r - \sum_j \xi_{rj} s_j) - k_{r,i}^r (s_i). \quad (5)$$

$$\frac{\partial s_i}{\partial t} = \frac{\partial N_i^T}{\partial t} + \sum_l \sum_k ^s R_{lk}^i. \quad (6)$$

The superficial permeation velocity \bar{v} through the porous fibrin matrix of the blood clot is given by Darcy's law:

$$\bar{v} = -K \nabla P, \quad (7)$$

where $K = k(x,y,t)/\mu$ for plasma of viscosity μ permeating through fibrin with a specific permeability k . For two dimensional calculations of \bar{v}_x and \bar{v}_y at every position and time, the Poisson equation of the form $\nabla \cdot \bar{v} = \nabla \cdot (K(x,y,t) \nabla P) = 0$ is solved with the hydraulic permeability (K) varying in space and time owing to lysis, but not dependent on the local direction of flow at a given position (2).

A particular challenge in modeling fibrinolysis is the complexity of solubilization as fibrin is degraded to a complex distribution of fragments. Heterogeneous reactions involving plasmin cleavage of fibrin will cause a decrease in solid fibrin volume due to solubilization. This class of reactions is commonly treated by a "shrinking-core" model, whereas the "progressive conversion" model is used for reaction systems that have no change in solid shape. During lysis, it is likely that both surface erosion and inner fiber dissolution occur simultaneously. However the relative extents are not known and may depend on specific reaction conditions. Surface erosion has been observed in collagen fibrils (104), whereas fibrin displays both surface erosion (Figure 3) and complex agglomeration and restructuring during lysis (Figure 4). Veklich et al (117) found, by electron microscopy, that fibrinolysis results in larger fragments with evidence for trans-

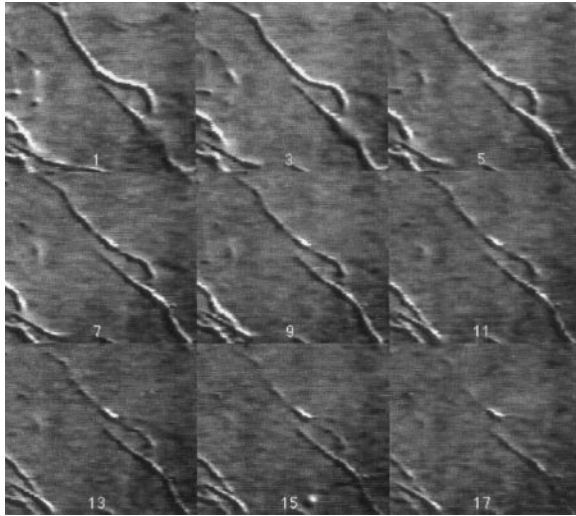


FIGURE 3 Lysis under shrinking-core conditions. Visualization by contrast-enhanced differential interference contrast microscopy shows the dissolution by 1- μ M plasmin of individual fibrin fibers adsorbed to a coverslip. Frames are shown every 10 s. Fibrin fibers were formed from 3 mg/ml of fibrinogen clotted with 1 U/ml of thrombin in 0.1 M NaCl.

verse cutting across fibers rather than uniform degradation of the outer radius of the fiber. Also, large fragments of fibrin have been eluted from dissolving fibrin (121). Anand & Diamond (3) assumed that the fiber is solubilized at constant density. With this approach the change in fiber diameter can be related to the historic amount of fibrin cleavage L at each position and time as

$$L(x',t') = \gamma \int_0^{t'} k_{\text{cat}} s_{\text{plasmin}}(x',t) dt, \quad (8)$$

where γ is equal to 0.1 corresponding to the solubilization of an equivalent of one monomer by 10 peptide cleavage events ($\gamma = 0.1$). This approach avoids the difficulty of calculating the dynamic spatial gradients for species within a micrometer-sized fiber that itself resides within a fibrin clot that has macroscopic dynamic spatial gradients.

To date, mathematical analyses of fibrinolysis tend to be subcases of Eq. 4–6. Approaches that neglect the $(s-c)\partial\varepsilon/\partial t$ term do not conserve mass and correspond to the assumption that species present within the dissolving fiber are completely degraded or inhibited and cannot rebind intact fibrin (31). Approaches that do not account for reversible adsorption and neglect the $(1-\varepsilon)\partial N^T/\partial t$ term are limited to treatments of soluble plasminogen activators such as uPA and streptokinase and use a fibrinolytic rate based on an effective active plasmin concentration (bound + soluble plasmin) (133, 134). Kolev et al (57) have conducted a moving-front analysis by assuming a constant thickness, thin reaction zone (due to adsorption-controlled penetration of diffusing plasmin) of the fibrin, which is separated from the bulk enzyme solution by a singular boundary. If front propagation is slow and does not travel very far for initially thin gel structures (relative

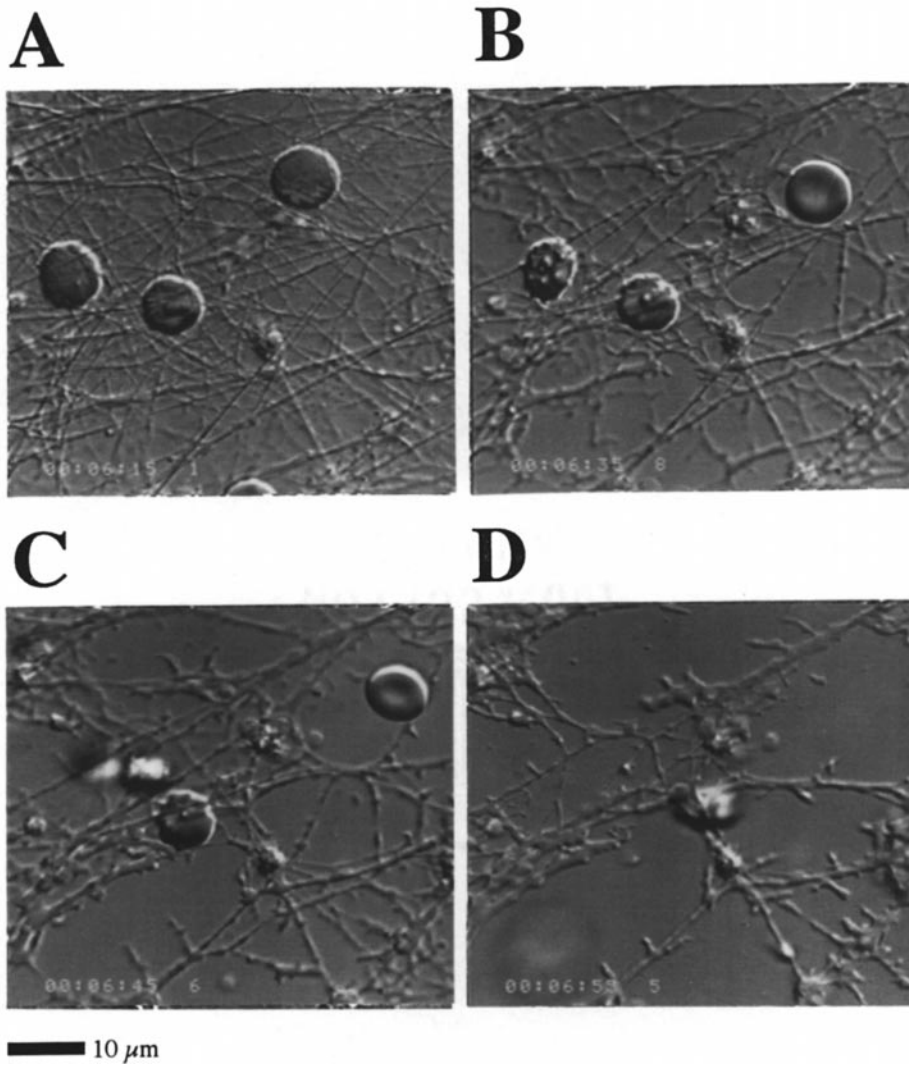


FIGURE 4 Fibrin fibers agglomerate together and undergo extremely complex conformational changes as the fibrous nature of the material is lost. Fibers were formed from recalcified human plasma and treated with 1- μM urokinase. Similar results are observed in purified fibrin. Images are shown at time equals 0 (a), 20s (b), 30s (c), and 40s (d) after addition of uPA.

to the time of enzyme diffusion), this assumption appears valid in the experiments of Kolev et al, whose results compared well with the full transport/reaction analysis of Anand & Diamond (3) and who calculated the instantaneous lysis rate as $R = (\gamma k_2) \cdot [\text{plasmin}_{\text{bound}}]$, where $\gamma k_2 = (0.1)5 \text{ s}^{-1} = 0.5 \text{ s}^{-1}$. Kolev found a similar apparent rate constant of 0.56 s^{-1} for lysis of fibrin formed in 100-mM

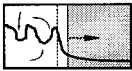
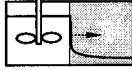
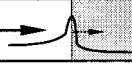
NaCl. Attempts to predict clot lysis without accounting for interstitial permeation by using various diffusion-controlled shrinking-core models and various progressive-conversion models failed to identify a single model to correlate lysis extents in patients (103).

Assay Methods and Boundary Conditions

Fibrin is an insoluble polymeric substrate, and this complicates the measurement of kinetics, thrombolytic activity, and prediction of clinical efficacy. In designing fibrinolytic assays to measure kinetics or to predict clinical efficacy, it is important to define the transport conditions and biochemistry of the fluid external to the fibrin gel (termed the extrinsic phase) as well as the transport of fluid within the fibrin (termed the intrinsic phase) (73, 91, 130, 132). Common lytic assays are shown in Table 3. The reaction processes may display a pseudo-steady state, but in reality every fibrinolytic assay is a batch reaction in which the fibrin may eventually be fully solubilized. If concentration gradients exist at the start of the assay (e.g. tPA in the extrinsic phase only) and the characteristic length of the clot is greater than $\sim 100 \mu\text{m}$, the role of transport processes will control the kinetics of lysis. For very thin films of fibrin ($< 100 \mu\text{m}$ thick) or dispersed fibrin suspensions (51, 129, 130), the systems are well mixed with rate processes dictated by heterogeneous enzyme kinetics only. Mixing of the extrinsic phase does not necessarily ensure adequate mixing at the fluid-gel boundary layer and will have no effect on transport inside the fibrin. Lysis front propagation is easily visualized and is a relevant predictor of thrombolytic efficacy. Chromogenic and fluorogenic substrates are very useful in probing the active site kinetics of purified enzymes and in calibrating enzymatic activity units (20, 63); however, the kinetic parameters give less insight into the heterogeneous rate processes of thrombolysis that involve adsorption and ternary complex assembly on fibrin.

Assays have also been developed to study lysis with laminar flow exposure of a surface of the clot, which typically enhances delivery to the surface (95). At a wall shear stress of 10 dyne/cm^2 (but not 5 dyne/cm^2), re-tPA and TNK-tPA both caused a dose-dependent removal of platelets adherent on preformed layer fibrin via a fibrinolytic mechanism (40). Komorowicz et al (58) found that increases in wall shear rate at a fibrin surface from 25 to 500 s^{-1} (0.25 to 5 dyne/cm^2) caused the rate of product release by circulating plasmin to increase 2.8-fold. This increase may be caused either by an increased removal rate of degrading fibrin (shear stress-enhanced embolization) or a reduction in transport limits across a concentration boundary layer with increasing flow. In an earlier study with whole-blood clots, plasma clots, fibrin gels, and partially compacted thrombi from Chandler loops, the effects of flowing liquid (citrate plasma or blood) over the clot surface tended to reduce the fibrinolytic activity of various plasminogen activators (74). This reduction was beyond explanation owing to the complexity of transport and cellular/plasma factors in the circulating fluid. Flow may perturb unique reactive environments near the clot surface.

TABLE 3 Transport issues in fibrinolytic assays^a

Assay	Advantage	Disadvantage
Stationary extrinsic phase 	<ul style="list-style-type: none"> •Simple •Can calibrate •96-well format •Can model 	<ul style="list-style-type: none"> •Diffusion limited kinetics •Rheological effects •Thick stagnant layer •Hard to sample reliably
Poorly mixed extrinsic phase 	<ul style="list-style-type: none"> •Suspended clots •Dynamic sampling •96-well plate/shaker •Fibrin film is gradientless 	<ul style="list-style-type: none"> •Lab to lab variability •Unknown external boundary layer thickness •Difficult to model
Well mixed extrinsic phase 	<ul style="list-style-type: none"> •No external phase transport limits •Dynamic removal and addition of fluid •May have steady state 	<ul style="list-style-type: none"> •Intrinsic phase diffusion limits •Low replicate numbers •Not commonly used
Controlled pressure drop 	<ul style="list-style-type: none"> •Replicates in vivo hemodynamics and therapy •Gives dynamic permeability •Can study pulsatility effects 	<ul style="list-style-type: none"> •Need advanced model •No true steady state •Permeation changes over time
Controlled velocity 	<ul style="list-style-type: none"> •Can vary from transport to reaction limited •Lytic fingering studies •Replicates in vivo transport 	<ul style="list-style-type: none"> •Need advanced model •Low replicate numbers •Need good clot adhesion •Hard to sample
Laminar flow extrinsic phase 	<ul style="list-style-type: none"> •Nonocclusive thrombi •Embolization studies •Rethrombosis studies •Good delivery to clot surface 	<ul style="list-style-type: none"> •Very complex physics •Difficult to model •Hard to assay •Boundary layer effects •Low replicate numbers
Well mixed fibrin suspension 	<ul style="list-style-type: none"> •Ideal for kinetic studies •Pseudohomogeneous •Dynamic removal/addition •Optical assays possible 	<ul style="list-style-type: none"> •Nonphysiologic substrate •Variability of substrate •Not predictive of thrombolytic drug delivery •Aggregation/wall adsorption

^aSchematic features include fibrin or clot (*shaded*), lysis front propagation (*dashed arrow*), fluid motion (*solid arrow*), mixing (*impeller*), concentration boundary layer (*dashed line*), and concentration profiles (*solid line*). A parabolic flow profile is indicated for the case of laminar flow extrinsic phase.

Diffusion-Mediated Lysis

In the absence of permeation, placement of lytic solutions adjacent to fibrin gels or blood clots will cause sharp lysis fronts to move across the structure. The velocity of these fronts depends on the concentration gradient for diffusion, the

enzymatic speed of fibrin degradation, and in some cases a rheological retraction mechanism (3, 94). Placement of human Glu₁-plasmin or Lys₇₇-plasmin adjacent to coarse fibrin (3 mg/ml) provided for a lysis front whose pseudo-steady-state velocity is given by the following (130, 131):

$$v_{\text{lysis}} \text{ (mm/min)} = 0.0164 [\text{plasmin}]^{0.4729} \text{ for } 0.01 < [\text{plasmin}] < 10 \text{ } \mu\text{M}.$$

Placement of uPA or tPA adjacent to coarse fibrin (3 mg/ml) containing 2.2- μM plasminogen causes lysis fronts to proceed at a pseudo-steady-state velocity as follows (130):

$$v_{\text{lysis}} \text{ (mm/min)} = 0.0715 [\text{uPA}]^{0.1936} \text{ for } 0.01 < [\text{uPA}] < 80 \text{ } \mu\text{M};$$

$$v_{\text{lysis}} \text{ (mm/min)} = 0.0551 [\text{tPA}]^{0.3384} \text{ for } 0.01 < [\text{tPA}] < 10 \text{ } \mu\text{M}.$$

Higher levels of tPA can actually reduce the speed of the lysis front through interference with plasmin activity (130). The presence of inhibitors and different levels of fibrin or plasminogen would change the above relationships. Under the most rapid lytic environments created in vitro, the fastest front velocity observed under conditions of diffusion was 0.16 mm/min (130).

At low enzyme concentrations of Lys₇₇-plasmin, uPA, or tPA of $<1 \mu\text{M}$, the experimentally measured lysis front position propagated proportionally to $t^{1/2}$. In computer simulations of lysis without convection, the position of the fibrinolysis front was proportional to $t^{1/2}$ as expected. However, at high enzyme concentrations (plasmin = 10 μM ; uPA or tPA $> 1 \mu\text{M}$), the measured front positions were correlated with t^1 and moved at nearly constant velocity and at speeds faster than simulated for diffusion-mediated transport (3), indicating non-Fickian behavior that is common to polymer dissolution (34). Anand & Diamond (3) demonstrated that fibrin fibers retracted under conditions of lysis in a region only a few micrometers away from the lysis front. The molecular origin of this retraction is not known. Similar retraction has been observed by confocal microscopy (94). It is not known whether these retraction mechanisms occur or contribute in the lysis of whole blood clots or retracted blood clots. Most lysis experiments with suspended whole blood clots in which diffusion is the major mode of transport take many hours to days to achieve 100% lysis, suggesting that a high lysis velocity ($>0.1 \text{ mm/min}$) is not achievable in these systems. In rigid gels, impaired retraction may participate to hinder lysis, as is observed with actin-laden fibrin (49) or Dusart's fibrin (29). Under permeation conditions that overwhelm retraction-mediated transport, there is no observed difference in lysis of fine and coarse gels (131).

Permeation-Enhanced Lysis

Permeation markedly enhances lysis of purified fibrin (130, 131), clotted plasma (1), clotted whole blood (12, 131), and retracted-blood clots (10, 134). Blinc et al (12) first demonstrated that a pressure head of 37 cm H₂O (27 mm Hg) across 3-cm-long blood clots ($\Delta P/L = 9.05 \text{ mm Hg/cm}$ of clot) caused a superficial

velocity of flowing plasma (viscosity ~ 1.32 centipoise at 22°C) of 6.7 ± 3.2 mm/min ($k = 1.22 \times 10^{-8}$ cm²). Lysis of these clots by diffusive delivery of uPA (500 IU) in plasma resulted in a lysis front velocity of 0.0083 mm/min. Pressure-driven permeation caused an 89% reduction in clot volume within 45 min, a 59-fold enhancement of lysis over diffusive delivery. However, permeation caused nonuniform lysis front and clot cannulation. The lysis front velocity at the center position of the clot was ~ 0.75 – 1.5 mm/min. For this lytic delivery regimen applied to unretracted-blood clots, the ratio v_{lysis}/\bar{v} was 0.15. Wu et al (131) found that permeation of $1\text{-}\mu\text{M}$ plasmin into unretracted-whole-blood clots caused lysis fronts to proceed at $v_{\text{lysis}}/\bar{v} \sim 0.25$ for permeation velocities from 0.05 to 1.4 mm/min. Although plasmin is normally impotent in plasma in suspended clot assays, the significant washout of antiplasmin as well as front loading of plasmin under permeation conditions can facilitate lysis of whole-blood clots.

For retracted clots treated with 400 IU/ml of uPA in plasma driven by $\Delta P/L = 14.6$ mm Hg/cm, nonuniform lysis fronts proceed at a velocity of ~ 0.1 mm/min (10, 134). The superficial permeation velocity was about 0.225 mm/min, and the ratio v_{lysis}/\bar{v} was 0.44. The lysis front was able to keep up reasonably well with the slowly moving permeation front despite the fact that local fibrin density was concentrated fivefold during retraction. In other studies with MRI to image the position of permeating fluid in retracted clots, Blinc et al (11) demonstrated that, under lytic conditions, the locations in a clot that experienced fluid permeation also experienced dissolution. Because $v_{\text{lysis}}/\bar{v} < 1$ for lysis of unretracted and retracted blood clots, increasing uPA or plasminogen in the permeating plasma would be expected to enhance the lysis rate.

In diluted plasma clots exposed to $0.1\ \mu\text{M}$ tPA and $1.0\ \mu\text{M}$ Glu-plasminogen permeating at constant velocities of 0.1 or 0.2 mm/min, the ratio of v_{lysis}/\bar{v} was about 1 in both cases (1), indicating that the lytic regime had sufficient or excess reactivity to keep pace with permeation. Increasing the tPA level in this experiment would not enhance the lysis front velocity.

Wu et al (131) studied the lysis of purified fibrin by plasmin or uPA under conditions of permeation. For permeation of $1\text{-}\mu\text{M}$ plasmin into 3 mg/ml of fine or coarse fibrin, $v_{\text{lysis}}/\bar{v} = 0.74$ for \bar{v} from 0.01 to 0.4 mm/min. For permeation of $1\text{-}\mu\text{M}$ uPA into 3 mg/ml of fine or coarse fibrin containing $2.2\text{-}\mu\text{M}$ Glu-plasminogen, $v_{\text{lysis}}/\bar{v} = 0.72$ for \bar{v} from 0.01 to 0.8 mm/min. These experiments represent relatively reactive lytic regimens in which the lysis front velocity kept pace with the permeation velocity. In contrast, for constant permeation of lower levels of plasmin at $\bar{v} = 0.1$ mm/min into 3 mg/ml of coarse fibrin, S.L. Diamond and V. Kudallur (data not shown) found a ratio of $v_{\text{lysis}}/\bar{v} = 0.42$ ($0.1\text{-}\mu\text{M}$ plasmin) and $v_{\text{lysis}}/\bar{v} = 0.1$ ($0.01\text{-}\mu\text{M}$ plasmin). For constant permeation of plasmin at $\bar{v} = 0.5$ mm/min into 3 mg/ml of coarse fibrin, S.L. Diamond and V. Kudallur (data not shown) found ratios of $v_{\text{lysis}}/\bar{v} = 0.72$ ($1\text{-}\mu\text{M}$ plasmin), $v_{\text{lysis}}/\bar{v} = 0.167$ ($0.1\text{-}\mu\text{M}$ plasmin), and $v_{\text{lysis}}/\bar{v} = 0.033$ ($0.01\text{-}\mu\text{M}$ plasmin). V. Kudallur and S.L. Diamond (data and computer simulations not shown) also concluded that increasing the concentration of fibrin to 6 or 9 mg/ml reduced the plasmin-mediated lysis

front velocity by two distinct mechanisms, enhanced fibrinolytic burden and feedback inhibition of plasmin by fibrin degradation products.

INTRAVENOUS LYTIC THERAPIES

Pharmacokinetics

Intravenous thrombolytic administration regimes for acute MI often involve a combination of bolus and continuous infusions. In the systemic circulation, changes in blood chemistry occur due to fibrin-independent plasminogen activation. Complex models with multiple half-lives for clearance and multiple compartments for tPA biodistribution, in physiologic and therapeutic settings, have been demonstrated to be highly accurate (26, 27). Chandler et al (27) found that tPA is cleared faster in subjects with low PAI-1 vs high PAI-1 levels ($t_{1/2}$ of 3.5 vs 5.4 min), owing to the slow clearance of the tPA–PAI-1 complex.

The dynamics of circulating plasminogen activators and associated changes in blood protein levels are dominated by the rate of hepatic clearance. Thus, a single-compartment model can accomplish a reasonably accurate description of changes in the systemic circulation (1, 109, 111). The concentration of each species (C_i , μM) in the systemic circulation is given by solution of a set of coupled ordinary differential equations that describe the rate of change of concentration of each species (C_i) in plasma (Eq. 8). The plasma of the circulation can be treated as a single, well-mixed compartment that can receive a user-specified infusion regime for any species $I_i(t)$ ($\mu\text{mol/s}$), and any species may be eliminated at a given rate by clearance $K_i(t)$ ($\mu\text{mol/s}$), as follows:

$$V_{\text{plasma}} \frac{dC_i}{dt} = V_{\text{plasma}} \sum_j \sum_k R^i(C_j, C_k) + I_i(t) - K_i(t). \quad (8)$$

In the circulatory system, the rate of generation (or loss) of the i th species $R^i(C_j, C_k)$ is determined by the reaction between the j th and k th species. The clearance rate of each species K_i is taken as a first-order process in C_i determined from the half-life of the species, where $K_i = (k C_i V_{\text{plasma}})$. (56, 108)

Pharmacodynamics

With in vitro kinetic data for the reaction network (Figure 1) and ex vivo arterial thrombi properties and initial plasma composition (Tables 1–2), Anand & Diamond (1) simulated an accelerated therapeutic regime for intravenous tPA therapy for coronary thrombolysis (122) involving a 15-mg bolus followed by infusion of 85 mg over 90 min. In the simulation, this regime provided for a relatively constant circulating level of tPA of about 0.04 μM (Figure 5A) during the first hour of therapy. Plasminogen dropped to less than half of its original level with the concomitant appearance of inhibited complexes. The lysis front advanced at

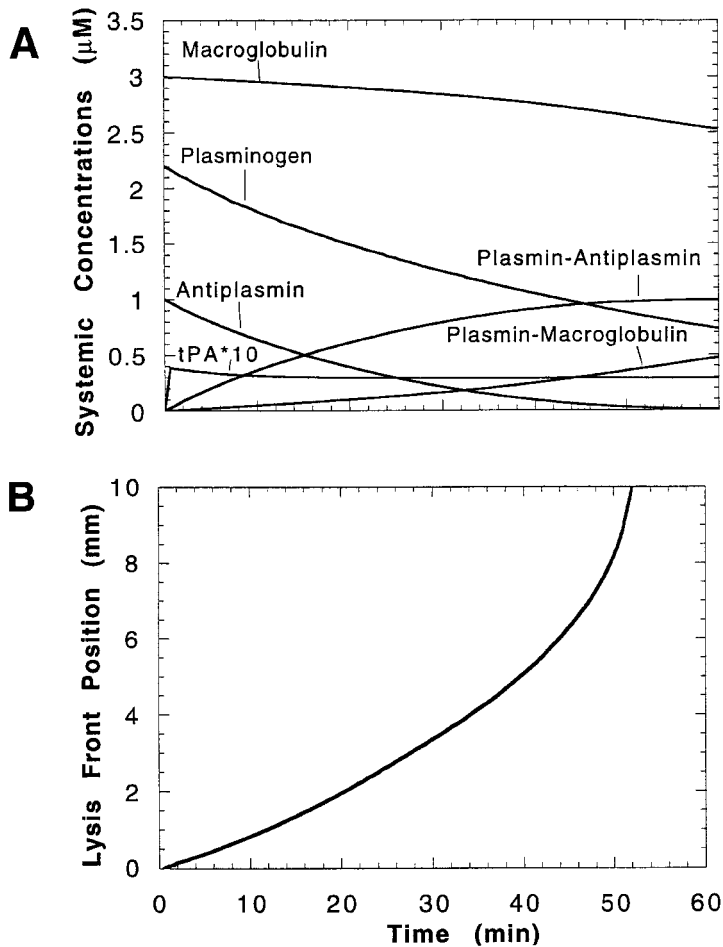


FIGURE 5 Lysis simulation of an arterial thrombus by intravenous tPA thrombolytic therapy (100-mg total dose). Changes in systemic species are shown (A) for a therapy initiated by a 15-mg tPA bolus followed by infusion of 85 mg of tPA over 90 min. Initial clot length is 1 cm, and initial pressure drop was set at 50 mm Hg/cm. Complete reperfusion is achieved at 52 min (B). Shown are the percent lysis profile (C) and concentration profiles of free and bound species (D–F) across the clot after 10 min of therapy. Used with permission from Anand & Diamond (1).

a nearly constant velocity of about 1 mm/10 min for the first 40 min of the therapy (Figure 5B), after which lysis proceeded more rapidly with the remaining 6 mm of the thrombi dissolving in the next 10 min. The prediction of clot lysis (with no adjustable parameters) is consistent with observed recanalization times between 45 and 90 min. At 10 min, dramatic changes in reactant concentrations

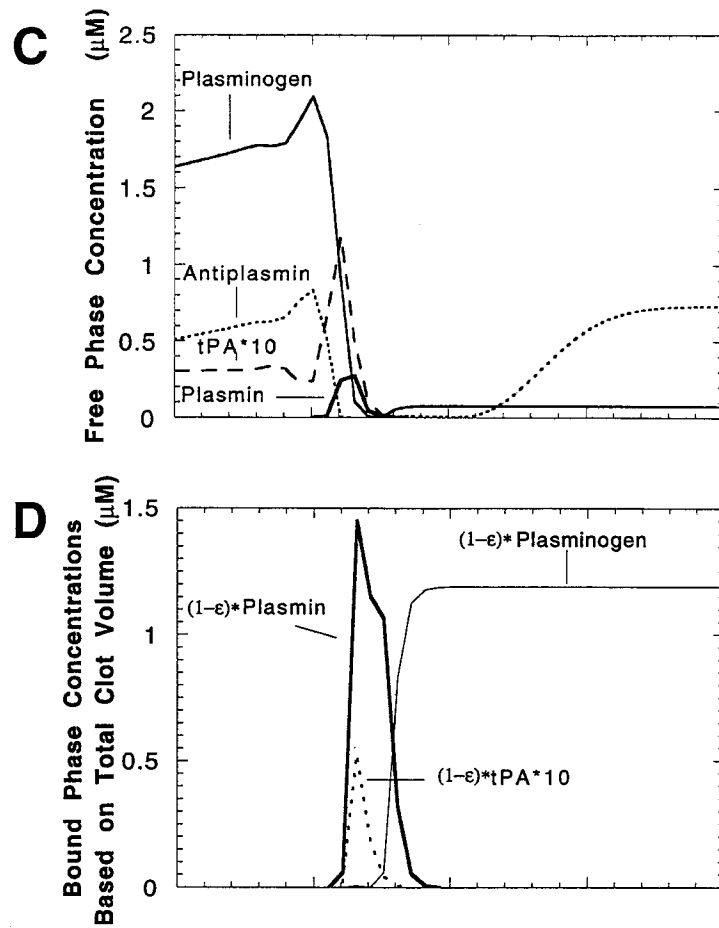


FIGURE 5 continued

were seen in a thin reaction zone (Figure 5C–E). The inhibited plasmin species moved with the permeating fluid through the lysis front. The overall thrombolytic rate (i.e. lysis front velocity) achieved as a result of this aggressive dosing scheme can be improved only marginally up to the point where the lysis front proceeds at a velocity comparable with the permeation velocity.

Simulation of i.v.-uPA (two-chain-uPA) therapy for acute MI for a protocol of a bolus of 8 mg uPA ($\sim 10^6$ IU abbokinase) followed by continuous infusion of 1 mg/h ($\sim 125,000$ IU/h) provided for an approximately constant level of 0.04- μM uPA (similar to the tPA level in Figure 6A). A zone of complete lysis proceeded about 1.5 mm across the front of the clot at 90 min. A low degree of lysis (5–30%) was present at 90 min in regions deep within the clot (0.2–1 cm). This

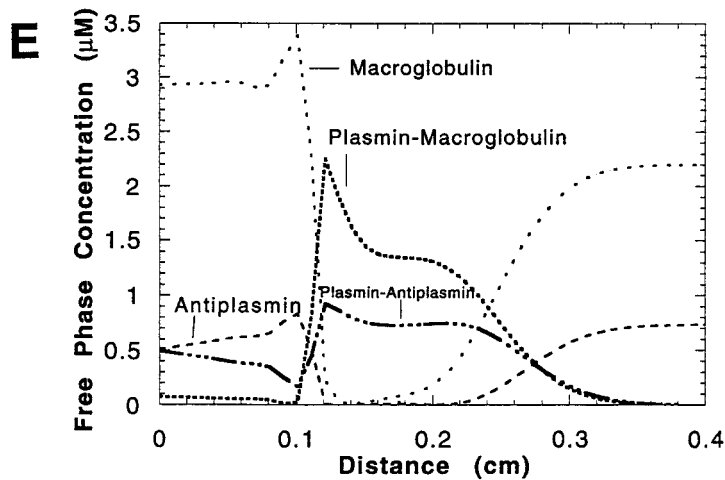


FIGURE 5 continued

deep zone of lysis was not seen with tPA and indicates that uPA activated an inner clot pool of plasminogen because its penetration into the clot was not slowed by binding. The distinct patterns of tPA and uPA thrombolysis make the deconvolution of additive vs synergistic biochemical effects of combined tPA/uPA i.v. therapies difficult.

CATHETER-BASED THERAPY

With intrathrombic delivery, penetration of the catheter into the clot causes compaction and disruption of the thrombus. For deep vein thrombosis, the facilitated delivery over the many centimeters of the clot justifies the approach because transport is insufficient for successful reperfusion via intravenous delivery.

A single-port catheter requires cannulation of the clot followed by continual infusion of the thrombolytic agent in conjunction with slow translation of the catheter through the thrombus (47, 67). Pulsatile pumping is a variation on this approach to enhance local mixing (53). Multiport catheters also require cannulation of the clot, but can deliver agent along the length of the clot with less need for adjustment of the catheter position. As the fluid leaving the catheter seeks the path of least resistance, the flow may not necessarily be evenly distributed across the ports unless careful design of the port diameter and port spacing is achieved. Similarly, porous balloons or porous membranes on catheter tips have been described. Catheter tips that contain numerous small ports at various angles help to generate high-speed jets of fluid rich in plasminogen activator (116). In this "pulse-spray" approach, benefits may be partly due to mechanical disruption and

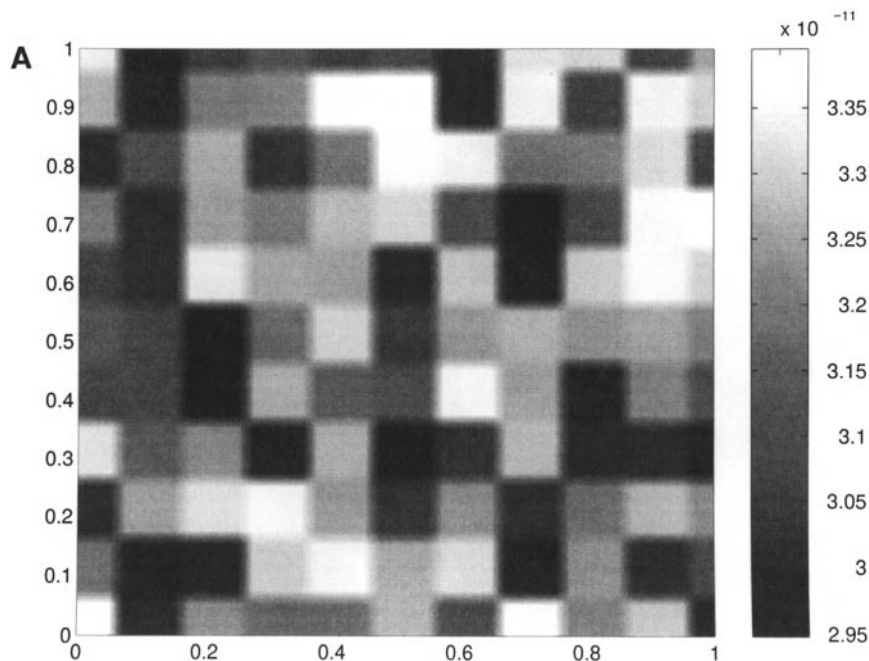


FIGURE 6 Lysis front progression at 10-min intervals ranging from 20 to 60 min for fibrin beds of increasing variability in local fibrin density and permeability. (*Panel above*) the initial permeability field had random variations in permeability around a baseline value (mid gray) of $3.16 \times 10^{-11} \text{ cm}^2$ (left). (*Panel opposite*) For fibrin with a 4% (A), 15% (B), or 25% (C) maximum variation in fibrin density, lysis fronts demonstrate the development of a lytic finger owing to increased random variations in local fibrin density (maximum permeability variation shown above each case). Used with permission from Anand & Diamond (2).

partly due to enhanced transport across a poorly mixed external boundary layer. The ability to actually force liquid radially from the catheter into the deeper layers of the clot is particularly difficult. The delivered fluid must follow the path of least resistance, typically the 100- to 1000- μm gap between the catheter and the thrombus, not the 1- to 10- μm pores of the blood clot. Thus, intrathrombic delivery is characterized by diffusive transport in the radial direction from the catheter surface across a few millimeters of clot toward the outer vessel wall. The low permeability of the vessel wall minimizes pressure-driven permeation in the radial direction. Kandarpa et al (52) found no difference between pulse-spray treatment and slow continuous infusion of uPA for peripheral thrombolysis.

Distinct from these drug-delivery catheters, several studies have demonstrated the use of the Bernoulli effect, in which fluid is forced from the catheter head

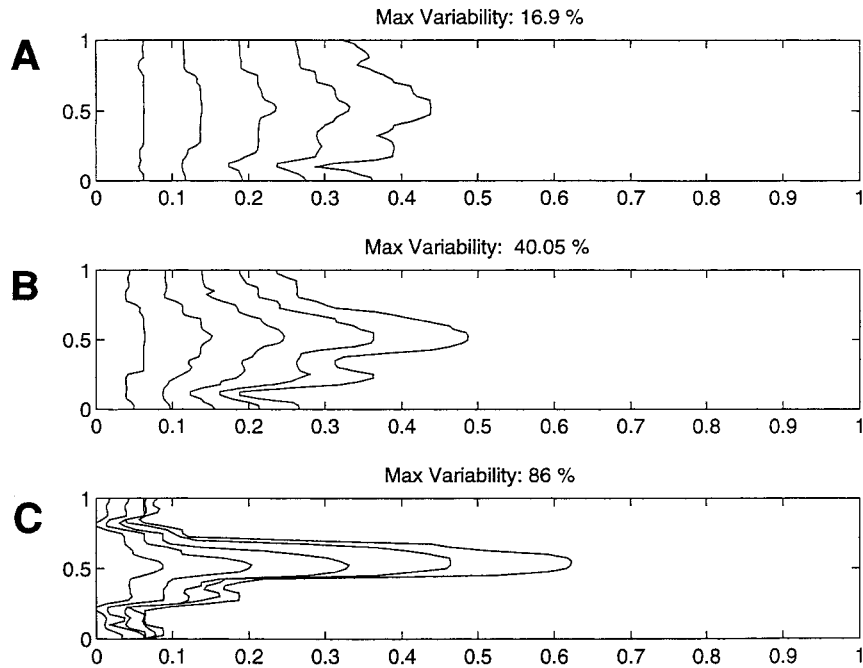


FIGURE 6 *continued*

and jets toward a receptacle lumen in the catheter to create a very low-pressure region (59, 120). This ‘‘rheolytic’’ approach causes recirculation vortices to perturb the thrombus in conjunction with forceful aspiration of the thrombus into the catheter. The approach is reported to remove the clot rapidly without the need for lytic agents, but does generate some hemolysis and local injury to the vessel wall (100).

Other physical enhancements of lysis include ultrasound and laser energy. Ultrasound, applied either externally or at the site of the catheter, can enhance the rate of thrombolysis via several distinct and interacting mechanisms (43). First, ultrasound-induced cavitation increases the specific permeability of fibrin (101). Unexpectedly, electron microscopy indicated that ultrasound caused thick fibers of fibrin to disaggregate into fine fibers (16). Transient openings of large pores in the presence of ultrasound are one possible reconciliation of the discrepant observations. Our laboratory has not observed by real-time microscopy any disaggregation in fiber structure during ultrasound exposure. Under conditions of constant pressure drop, lysis of clots exposed to ultrasound will be enhanced simply by enhancing permeation. However, ultrasound enhancements have also been observed under no-flow circumstances (107) or under constant velocity

permeation as measured in our laboratory. Consistent with ultrasound-induced structural changes in fibrin, there is a 40% increase in the binding of tPA to ultrasound-exposed fibrin (102). Ultrasound with cavitation or added microbubbles causes microstreaming to facilitate transport across the poorly mixed boundary layer at the clot/fluid boundary. It is not known whether significant microstreaming can occur within the pore space of fibrin, where viscous damping by the fiber surfaces would be significant. The use of lasers to ablate thrombus has received some attention (61, 110). Difficulty in complete dissolution is a challenge with this approach. Also, the thrombogenicity of charred residuals may be significant. The use of laser energy to drive drug-laden microspheres several hundred micrometers into an *in vitro* thrombus represents a novel approach to combine lasers with pharmacological agents (98).

DESIGNING LYTIC FORMULATIONS

Much emphasis has been placed on the molecular design of plasminogen activators to alter half-life and minimization of fibrin-independent plasminogen activation. For example, TNK-tPA has a longer circulatory half-life and causes little systemic activation, allowing a simpler, front-loaded bolus of the agent (54). In contrast, reteplase has a moderately reduced affinity of fibrin which allows for deeper penetration into a clot structure in a permeation assay (36), as would be predicted for lower-affinity agents and potentially with less interference with plasmin as seen with tPA (130). Madison (65) has provided an extensive review of the site-directed mutagenesis of tPA.

Multicomponent formulations of plasminogen activators have been developed but have not reached widespread clinical use. Although formulations may provide drug delivery scenarios not possible with a single protein, the issues of transport become significant for formulations that reduce plasminogen activator mobility. A two-step targeting approach with an antifibrin antibody conjugated with a non-blocking anti-uPA antibody has been reported to help target and enhance the activity of subsequently delivered uPA (96). Streptokinase has also been conjugated via avidin-biotin to RBCs (71), which allows for a long circulatory half-life of the plasminogen activator. A two-part formulation involving antifibrin antibody linked to heparin (anionic) in an electrostatic complex with cationic peptide-conjugated uPA has been demonstrated *in vitro*. This system allows triggered release by protamine of the cationic uPA conjugate because protamine has high-affinity binding to heparin (21). Such a system provides clot targeting by the antibody followed by triggered release of uPA, which would then have good motility in the fluid permeating through the clot. Also liposomes containing streptokinase (72) or tPA (45) or with surface-associated plasminogen (46) have been described to provide preferential delivery to a clot. Vakkalanka et al (115) have developed a temperature- and pH-sensitive polymer that undergoes swelling to provide enhanced release of streptokinase.

CLOT CANNULATION

In many circumstances, lysis proceeds across an occlusion in a nonuniform manner in which a lytic finger dissolves its way through the structure. The highly thrombogenic surfaces of cannulated clots, when exposed to flowing blood, would be prone to rethrombosis. Highly aggressive lytic regimes may also be associated with higher rates of lytic fingering. Studies have shown that higher doses of recombinant single-chain tPA can lead to reduced patency rates (41, 70). MRI visualization demonstrated that fluid permeation through a clot may be nonuniform (12). Zidansek et al (134) first modeled fingering lysis by using single-phase, multicomponent convection-diffusion-reaction equations solved with a lattice random-walk approach for various characteristic reaction times. The reaction time is a lumped parameter corresponding to the time between first arrival of lytic species and complete solubilization at a position. Such an approach is valid for a fluid-phase plasminogen activator, although an a priori prediction of the reaction time is not direct. Anand & Diamond (2) solved the biphasic equation of transport for the adsorbing- and reactive-species plasmin permeating through fibrin. In this approach, the relationship of enzyme properties, material properties, and transport parameters was directly related to front propagation and fingering.

In two-dimensional simulations of lysis in fibrin with initial variations in density, the plasmin concentration profiles and the lysis front shape revealed that the fingers progressed fastest in regions where the initial permeability was highest and therefore provided for enhanced plasmin transport. Anand & Diamond (2) found that increasing the variability of the initial fibrin density resulted in increasing the size of the lytic fingers (Figure 6). Anand & Diamond (2) concluded that there are distinct mechanisms by which dissolution fingers can exist:

(1) Structural: a blood clot is formed by the random aggregation of fibrin bundles under flow. These bundles are typically oriented with some degree of randomness and with various pore diameters and hence would lead to an initial permeability field varying considerably in space;

(2) Rheological: Pressure-driven permeation would lead to deformation of the proximal face of a clot, resulting in enhanced velocities through the middle of the blood clot;

(3) Cellular: Platelet retraction may result in less fibrin fibers present in the middle of the clot, leading to higher velocities in this region.

SUMMARY

1. Pressure-driven permeation controls the rate of drug penetration into a dissolving thrombus. Under conditions of extremely rapid lysis in which transport is rate limiting, the lysis front proceeds at essentially the velocity of the permeating fluid (or slightly faster owing to dispersional processes). This estab-

lishes the theoretical maximum rate of lysis. Under conditions of only diffusive delivery and extremely rapid lysis reactions, the maximum lysis front velocity is about 0.15 mm/min. This velocity is achieved through fiber retraction enhancement of transport, which may not be operative in rigid or dense structures.

2. Plasminogen activators with high affinity will bind and accumulate on the proximal face of the thrombus with local concentrations considerably higher than in the bulk extrinsic phase. Lower-affinity agents will have significantly better penetration into the clot under conditions of permeation to activate interior pools of plasminogen.
3. Protein diffusion is not significantly hindered in the pore space of fibrin.
4. Fibrinolysis is fundamentally heterogeneous and transient. Kinetic assays that begin with macroscopic fibrin or clot structures and have a defined intrinsic phase and extrinsic phase produce kinetic parameters with lumped diffusion-limited or mixing contributions.
5. Small fluctuations of the local fibrin density can create preferred paths of permeation and result in clot cannulation or embolism. After clot cannulation, lysis proceeds significantly more slowly and is controlled by diffusion in the radial direction.
6. Catheter delivery of plasminogen activators faces some of the same transport challenges as i.v. therapies. Attempts at direct pumping of buffer into a thrombus will result in significant leakage and limited deep penetration because the fluid, always taking the path of least resistance, will explore the open flow paths between the catheter and the thrombus instead of penetrating into the thrombus. Ultrasound has molecular effects on fibrin structure, permeability, and fibrinolytic biochemistry without direct "pumping" of unidirectional solvent flow into the fibrin.

Visit the Annual Reviews home page at <http://www.AnnualReviews.org>.

ACKNOWLEDGMENTS

This work was supported by National Institutes of Health grants R01 HL-56621 and R42 HL-60468. The author is an established investigator of the National American Heart Association. The principal investigator would like to thank Drs. Sriram Anand, Venkat Kudallur, and Jung He Wu for important contributions toward understanding the bioengineering analysis of thrombolysis.

LITERATURE CITED

1. Anand S, Diamond SL. 1995. A computer simulation of systemic circulation and clot lysis dynamics during thrombolytic therapy that accounts for inner clot transport and reaction. *Circulation* 94:763-74

2. Anand S, Diamond SL. 1997. Mechanisms by which thrombolytic therapy results in nonuniform lysis and residual thrombus after reperfusion. *Ann. Biomed. Eng.* 25:964–74
3. Anand S, Wu JH, Diamond SL. 1995. Enzyme-mediated proteolysis of fibrous biopolymers: dissolution front movement in fibrin and collagen under conditions of diffusive and convective transport. *Biotechnol. Bioeng.* 48:89–107
4. Araie E, Fujita M, Ohno A, Ejiri M, Yamanishi K, et al. 1992. Relationship between the preexistent coronary collateral circulation and successful intracoronary thrombolysis for acute myocardial infarction. *Am. Heart J.* 123(6):1452–55
5. Bale MD, Ferry JD. 1988. Strain enhancement of elastic modulus in fine fibrin clots. *Thromb. Res.* 52(6):565–72
6. Basmadjian D. 1984. The hemodynamic forces acting on thrombi, from incipient attachment of single cells to maturity and embolization. *J. Biomech.* 17(4):287–98
7. Bear J, Bachmat Y. 1991. *Introduction to Modeling of Transport Phenomena in Porous Media*. Dordrecht, the Netherlands: Kluwer. 553 pp.
8. Bini A, Callender S, Procyk R, Blomback B, Kudryk BJ. 1994. Flow and antibody binding properties of hydrated fibrins prepared from plasma, platelet rich plasma and whole blood. *Thromb. Res.* 76(2):145–56
9. Blinc A, Francis CW. 1996. Transport processes in fibrinolysis and fibrinolytic therapy. *Thromb. Haemost.* 76(4):481–91
10. Blinc A, Keber D, Lahajnar G, Stegnar M, Zidansek A, Demsar F. 1992. Lysing patterns of retracted blood clots with diffusion or bulk flow transport of plasma with urokinase into clots—a magnetic resonance imaging study in vitro. *Thromb. Haemost.* 68:667–71
11. Blinc A, Kennedy SD, Bryant G, Marder VJ, Francis CW. 1994. Flow through clots determines the rate and pattern of fibrinolysis. *Thromb. Haemost.* 71:230–35
12. Blinc A, Planinsic G, Keber D, Jarh O, Lahajnar G, et al. 1991. Dependence of blood clot lysis on the mode of transport of urokinase into the clot: a magnetic resonance imaging study in vitro. *Thromb. Haemost.* 65:549–52
13. Blomback B, Carlsson K, Fatah K, Hessel B, Procyk R. 1994. Fibrin in human plasma: gel architectures governed by rate and nature of fibrinogen activation. *Thromb. Res.* 75(5):521–38
14. Blomback B, Carlsson K, Hessel B, Liljeborg A, Procyk R, Aslund N. 1989. Native fibrin gel networks observed by 3D microscopy, permeation and turbidity. *Biochim. Biophys. Acta* 997(1–2):96–110
15. Booth NA, Robbie LA, Croll AM, Bennett B. 1992. Lysis of platelet-rich thrombi: the role of PAI-1. *Ann. NY Acad. Sci.* 667:70–80
16. Braaten JV, Goss RA, Francis CW. 1997. Ultrasound reversibly disaggregates fibrin fibers. *Thromb. Haemost.* 78(3):1063–68
17. Braaten JV, Jerome WG, Hantgan RR. 1994. Uncoupling fibrin from integrin receptors hastens fibrinolysis at the platelet-fibrin interface. *Blood* 83:982–93
18. Brenner H, Gaydos LJ. 1977. The constrained Brownian movement of spherical particles in cylindrical pores of comparable radius. *J. Colloid Interface Sci.* 58:312–55
19. Brommer EJP, van Loon BJP, Rijken DC, Van Bockel JH. 1992. Composition and susceptibility to thrombolysis of pathological human arterial thrombi. *Ann. NY Acad. Sci.* 667:283–85
20. Butenas S, DiLorenzo ME, Mann KG. 1997. Ultrasensitive fluorogenic substrates for serine proteases. *Thromb. Haemost.* 78(4):1193–201
21. Byun Y, Yang VC. 1998. Delivery system for targeted thrombolysis without the

- risk of hemorrhage. *Am. Soc. Artif. Intern Organs* 44(5):M638–41
22. Carr ME. 1988. Fibrin formed in plasma is composed of fibers more massive than those formed from purified fibrinogen. *Thromb. Haemost.* 59(3):535–39
 23. Carr ME Jr, Alving BM. 1995. Effect of fibrin structure on plasmin-mediated dissolution of plasma clots. *Blood Coagul. Fibrinolysis* 6(6):567–73
 24. Carr ME Jr, Hardin CL. 1987. Fibrin has larger pores when formed in the presence of erythrocytes. *Am. J. Physiol.* 253(5):H1069–73
 25. Carr ME Jr, Shen LL, Hermans J. 1977. Mass-length ratio of fibrin fibers from gel permeation and light scattering. *Biopolymers* 16(1):1–15
 26. Chandler WL, Alessi MC, Aillaud MF, Henderson P, Vague P, Juhan-Vague I. 1997. Clearance of tissue plasminogen activator (tPA) and tPA/plasminogen activator inhibitor type 1 (PAI-1) complex: relationship to elevated tPA antigen in patients with high PAI-1 activity levels. *Circulation* 96(3):761–68
 27. Chandler WL, Levy WC, Veith RC, Stratton JR. 1993. A kinetic model of the circulatory regulation of tissue plasminogen activator during exercise, epinephrine infusion, and endurance training. *Blood* 81(12):3293–302
 28. Charney R, Cohen M. 1993. The role of the coronary collateral circulation in limiting myocardial ischemia and infarct size. *Am. Heart J.* 126(4):937–45
 29. Collet JP, Woodhead JL, Soria J, Soria C, Mirshahi M, et al. 1996. Fibrinogen Dusart: Electron microscopy of molecules, fibers and clots, and viscoelastic properties of clots. *Biophys. J.* 70(1):500–10
 30. Cross DT III, Moran CJ, Akins PT, Angtuaco EE, Derdeyn CP, Diringer MN. 1998. Collateral circulation and outcome after basilar artery thrombolysis. *Am. J. Neuroradiol.* 19(8):1557–63
 31. Diamond SL, Anand S. 1993. Inner clot diffusion and permeation during fibrinolysis. *Biophys. J.* 65:2622–43
 32. Di Stasio E, Nagaswami C, Weisel JW, Di Cera E. 1998. Cl⁻ regulates the structure of the fibrin clot. *Biophys. J.* 75(4):1973–79
 33. Dullien FA. 1979. *Porous Media: Fluid Transport and Pore Structure*. New York: Academic. 167 pp.
 34. Edwards DA, Cohen DS. 1995. A mathematical model for a dissolving polymer. *AIChE J.* 41:2345–55
 35. Fatah K, Silveira A, Tornvall P, Karpe F, Blomback M, Hamsten A. 1996. Prone to formation of tight and rigid fibrin gel structures in men with myocardial infarction at a young age. *Thromb. Haemost.* 76(4):535–40
 36. Fischer S, Kohnert U. 1997. Major mechanistic differences explain the higher clot lysis potency of reteplase over alteplase: lack of fibrin binding is an advantage for bolus application of fibrin specific thrombolytics. *Fibrinolysis Proteolysis* 11:129–35
 37. Gabriel DA, Muga K, Boothroyd EM. 1992. The effect of fibrin structure on fibrinolysis. *J. Biol. Chem.* 267(34):24259–63
 38. Garber PJ, Mathieson AL, Ducas J, Patton JN, Geddes JS, Prewitt RM. 1995. Thrombolytic therapy in cardiogenic shock: effect of increased aortic pressure and rapid tPA administration. *Can. J. Cardiol.* 11:30–36
 39. Glover CJ, McIntire LV, Brown CH III, Natelson EA. 1975. Dynamic coagulation studies: influence of normal and abnormal platelets on clot structure formation. *Thromb. Res.* 7(1):185–98
 40. Graham DA, Huang TC, Keyt BA, Alevisiadou BR. 1998. Real-time measurement of lysis of mural platelet deposits by fibrinolytic agents under arterial flow. *Ann. Biomed. Eng.* 26(4):712–24
 41. Gurbel PA, Anderson RD, Maccord CS, Scott H, Serebruany V, Herzog WR. 1994. Accelerated intravenous dosing of

- recombinant tissue type plasminogen activator causes rapid but unstable reperfusion in a canine model of acute myocardial infarction. *Coron. Artery Dis.* 5:929–36
42. Hantgan RR, Francis CW, Marder VJ. 1994. Fibrinogen structure and physiology. In *Hemostasis and Thrombosis: Basic Principles and Clinical Practice*, ed. RW Colman, J Hirsh, VJ Marder, EW Salzman, pp. 277–300. Philadelphia, PA: Lippincott. 3rd ed.
43. Harpaz D, Chen XC, Francis CW, Meltzer RS. 1994. Ultrasound accelerates urokinase-induced thrombolysis and reperfusion. *Am. Heart J.* 127(5):1211–19
44. Harpel PC, Chang TS, Verderber E. 1985. Tissue plasminogen activator and urokinase mediate the binding of glu-plasminogen to plasma fibrin. I. Evidence for new binding sites in plasmin-degraded fibrin I. *J. Biol. Chem.* 260:4432–40
45. Heeremans JL, Prevost R, Bekkers ME, Los P, Emeis JJ, et al. 1995. Thrombolytic treatment with tissue-type plasminogen activator (t-PA) containing liposomes in rabbits: a comparison with free t-PA. *Thromb. Haemost.* 73(3):488–94
46. Heeremans JL, Prevost R, Feitsma H, Kluft C, Crommelin DJ. 1998. Clot accumulation characteristics of plasminogen-bearing liposomes in a flow-system. *Thromb. Haemost.* 79(1):144–49
47. Hess H, Ingrisch H, Mietaschk A, Rath H. 1982. Local low-dose thrombolytic therapy of peripheral arterial occlusions. *N. Engl. J. Med.* 307(26):1627–30
48. Jackson GW, James DF. 1986. The permeability of fibrous porous media. *Can. J. Chem. Eng.* 64:364–74
49. Janmey PA, Lamb JA, Ezzell RM, Hvidt S, Lind SE. 1992. Effects of actin filaments on fibrin clot structure and lysis. *Blood* 80(4):928–36
50. Johnson EM, Berk DA, Jain RK, Deen WM. 1996. Hindered diffusion in agarose gels: test of effective medium model. *Biophys. J.* 70:1017–26
51. Kanai S, Okamoto H, Tamaura Y, Yamazaki S, Inada Y. 1979. Fibrin suspensions as a substrate for plasmin: determination of kinetics. *Thromb. Haemost.* 42:1153–58
52. Kandarpa K, Chopra PS, Aruny JE, Polak JF, Donaldson MC, et al. 1993. Intraarterial thrombolysis of lower extremity occlusions: prospective, randomized comparison of forced periodic infusion and conventional slow continuous infusion. *Radiology* 188(3):861–67
53. Kandarpa K, Drinker PA, Singer SJ, Caramore D. 1988. Forceful pulsatile local infusion of enzyme accelerates thrombolysis: in vivo evaluation of a new delivery system. *Radiology* 168(3):739–44
54. Keyt BA, Paoni NF, Refino CJ, Berleau L, Nguyen H, et al. 1994. A faster-acting and more potent form of tissue plasminogen activator. *Proc. Natl. Acad. Sci. USA* 91(9):3670–74
55. Kirkner DJ, Theis TL, Jennings AA. 1984. Multicomponent solute transport with sorption and soluble complexation. *Adv. Water Res.* 7:121–25
56. Kohler M, Sen S, Miyashita C, Hermes R, Pindur G, et al. 1991. Half-life of single chain urokinase-type plasminogen activator (scu-PA) and two-chain urokinase-type plasminogen activator (tcu-PA) in patients with acute myocardial infarction. *Thromb. Res.* 62:75–81
57. Kolev K, Tenekedjiev K, Komorowicz E, Machovich R. 1997. Functional evaluation of the structural features of proteases and their substrate in fibrin surface degradation. *J. Biol. Chem.* 272(21):13666–75
58. Komorowicz E, Kolev K, Lerant I, Machovich R. 1998. Flow rate-modulated dissolution of fibrin with clot-embedded and circulating proteases. *Circ. Res.* 82(10):1102–8
59. Koning R, Cribier A, Gerber L, Eltchaninoff H, Tron C, et al. 1997. A new

- treatment for severe pulmonary embolism: percutaneous rheolytic thrombectomy. *Circulation* 96(8):2498–500
60. Kuntamukkula MS, McIntire LV, Moake JL, Peterson DM, Thompson WJ. 1978. Rheological studies of the contractile force within platelet-fibrin clots: effects of prostaglandin E1, dibutyryl-cAMP and dibutyryl-cGMP. *Thromb. Res.* 13(6):957–69
61. Labs JD, Caslowitz PL, White RI Jr, Anderson JH, Williams GM. 1991. Experimental treatment of thrombotic vascular occlusion. *Lasers Surg. Med.* 11(4):363–71
62. Lijnen HR, Van Hoef B, Collen D. 1991. On the reversible interaction of plasminogen activator inhibitor-1 with tissue-type plasminogen activator and with urokinase-type plasminogen activator. *J. Biol. Chem.* 266:4041–44
63. Lottenberg R, Christensen U, Jackson CM, Coleman PL. 1981. Assay of coagulation proteases using peptide chromogenic and fluorogenic substrates. *Methods Enzymol.* 80:341–61
64. Lucas MA, Fretto LJ, McKee PA. 1983. The binding of human plasminogen to fibrin and fibrinogen. *J. Biol. Chem.* 258:4249–56
65. Madison EL. 1994. Probing structure-function relationships of tissue-type plasminogen activator by site-specific mutagenesis. *Fibrinolysis* 8:221–36
66. Matveyev MY, Domogatsky SP. 1992. Penetration of macromolecules into contracted blood clots. *Biophys. J.* 63:862–63
67. McNamara TO, Fischer JR. 1985. Thrombolysis of peripheral arterial and graft occlusions: improved results using high-dose urokinase. *Am. J. Roentgenol.* 144(4):769–75
68. Miller RD, Burchell HB, Edwards JE. 1951. Myocardial infarction with and without acute coronary occlusion: a pathological study. *Arch. Intern. Med.* 88:597–611
69. Mizuno K, Satomura K, Miyamoto A, Arakawa K, Shibuya T, et al. 1992. Angioscopic evaluation of coronary-artery thrombi in acute coronary syndromes. *N. Engl. J. Med.* 326:287–91
70. Mueller HS, Rao AK, Forman SA, TIMI Investigators. 1987. Thrombolysis in myocardial infarction (TIMI): comparative studies of coronary reperfusion and systemic fibrinolysis with two forms of recombinant tissue-type plasminogen activator. *J. Am. Coll. Cardiol.* 10:479–90
71. Muzykantov VR, Sakharov DV, Smirnov MD, Samokhin GP, Smirnov VN. 1986. Immunotargeting of erythrocyte-bound streptokinase provides local lysis of a fibrin clot. *Biochim. Biophys. Acta* 884(2):355–62
72. Nguyen PD, O'Rear EA, Johnson AE, Patterson E, Whitsett TL, Bhakta R. 1990. Accelerated thrombolysis and reperfusion in a canine model of myocardial infarction by liposomal encapsulation of streptokinase. *Circ. Res.* 66(3):875–78
73. Nishino N, Kakkar VV, Scully MF. 1991. Influence of intrinsic and extrinsic plasminogen upon the lysis of thrombi in vitro. *Thromb. Haemost.* 66(6):672–77
74. Nishino N, Scully MF, Rampling MW, Kakkar VV. 1990. Properties of thrombolytic agents in vitro using a perfusion circuit attaining shear stress at physiological levels. *Thromb. Haemost.* 64(4):550–55
75. Nitsche JM, Balgi G. 1994. Hindered Brownian diffusion of spherical solutes within circular cylindrical pores. *Ind. Eng. Chem. Res.* 33:2242–47
76. Novak CF, Schechter RS, Lake LW. 1989. Diffusion and solid dissolution/precipitation in permeable media. *AIChE J.* 35:1057–72
77. Ogston AG, Preston BN, Wells JD. 1973. On the transport of compact particles through solutions of chain polymers. *Proc. R. Soc. London Ser. A* 333:297–316

78. Palabrica T, Lobb R, Furie BC, Aronovitz M, Benjamin C, et al. 1992. Leukocyte accumulation promoting fibrin deposition is mediated in vivo by P-selectin on adherent platelets. *Nature* 359(6398):848–51
79. Peppas NA, Wu JC, von Meerwall ED. 1994. Mathematical modeling and experimental characterization of polymer dissolution. *Macromolecules* 27:5626–41
80. Perez-Castellano N, Garcia EJ, Abeytua M, Soriano J, Serrano JA, et al. 1998. Influence of collateral circulation on in-hospital death from anterior acute myocardial infarction. *J. Am. Coll. Cardiol.* 31(3):512–18
81. Phillips RJ, Deen WM, Brady JF. 1989. Hindered transport of spherical macromolecules in fibrous membranes and gels. *AIChE J.* 35:1761–69
82. Potter van Loon BJP, Rijken DC, Brommer EJP, van der Maas APC. 1992. The amount of plasminogen, tissue-type plasminogen activator, and plasminogen activator inhibitor type 1 in human thrombi and the relation to ex-vivo lysis. *Thromb. Haemost.* 67:101–5
83. Prewitt RM. 1993. Thrombolytic therapy in patients where hypotension and cardiogenic shock complicate acute myocardial infarction. *Can. J. Cardiol.* 9: 155–57
84. Prewitt RM, Downes AM, Gu SA, Chan SM, Ducas J. 1991. Effects of hydralazine and increased cardiac output on recombinant tissue plasminogen activator-induced thrombolysis in canine pulmonary embolism. *Chest* 99:708–14
85. Prewitt RM, Gu S, Garber PJ, Ducas J. 1992. Marked systemic hypotension depresses coronary thrombolysis induced by intracoronary administration of recombinant tissue-type plasminogen activator. *J. Am. Coll. Cardiol.* 20:1626–33
86. Prewitt RM, Gu S, Schick U, Ducas J. 1994. Intraaortic balloon counterpulsation enhances coronary thrombolysis induced by intravenous administration of a thrombolytic agent. *J. Am. Coll. Cardiol.* 23:794–98
87. Prewitt RM, Gu S, Schick U, Wiens A, Ducas J. 1993. The effect of a moderate increase in a low coronary artery inflow pressure on coronary thrombolysis induced by intravenous administration of recombinant tissue plasminogen activator. *Thromb. Haemost.* 69:1353 (Abstr. 2913)
88. Prewitt RM, Gu SA, Greenberg D, Chan SM, Schick U, et al. 1991. Effects of flow on recombinant tissue plasminogen activator-induced pulmonary thrombolysis. *J. Appl. Physiol.* 71:1441–46
89. Robbie LA, Young SP, Bennett B, Booth NA. 1997. Thrombi formed in a Chandler loop mimic human arterial thrombi in structure and PAI-1 content and distribution. *Thromb. Haemost.* 77(3):510–15
90. Roberts WW, Kramer O, Rosser RW, Nestler FH, Ferry JD. 1974. Rheology of fibrin clots. I. Dynamic viscoelastic properties and fluid permeation. *Biophys. Chem.* 1(3):152–60
91. Sabovic M, Lijnen HR, Keber D, Collen D. 1989. Effect of retraction on the lysis of human clots with fibrin specific and non-fibrin specific plasminogen activators. *Thromb. Haemost.* 62:1083–87
92. Sahimi M, Hughes BD, Scriven LE, Davis HT. 1986. Dispersion in flow through porous media—one-phase flow. *Chem. Eng. Sci.* 41:2103–22
93. Sakharov DV, Domogatsky SP, Rijken DC. 1994. An experimental system for investigation of penetration of components of the fibrinolytic system into a plasma clot. *Fibrinolysis* 8:116–19
94. Sakharov DV, Nagelkerke JF, Rijken DC. 1996. Rearrangements of the fibrin network and spatial distribution of fibrinolytic components during plasma clot lysis. Study with confocal microscopy. *J. Biol. Chem.* 271(4):2133–38
95. Sakharov DV, Rijken DC. 1995. Super-

- ficial accumulation of plasminogen during plasma clot lysis. *Circulation* 92(7): 1883–90
96. Sakharov DV, Sinitsyn VV, Kratasjuk GA, Popov NV, Domogatsky SP. 1988. Two-step targeting of urokinase to plasma clot provides efficient fibrinolysis. *Thromb. Res.* 49(5):481–88
 97. Savage B, Saldivar E, Ruggeri ZM. 1996. Initiation of platelet adhesion by arrest onto fibrinogen or translocation on von Willebrand factor. *Cell* 84(2): 289–97
 98. Shangguan HQ, Gregory KW, Casperson LW, Prahl SA. 1998. Enhanced laser thrombolysis with photomechanical drug delivery: an in vitro study. *Lasers Surg. Med.* 23(3):151–60
 99. Shapiro M, Brenner H. 1988. Dispersion of a chemically reactive solute in a spatially periodic model of a porous medium. *Chem. Eng. Sci.* 43:551–57
 100. Sharafuddin MJ, Hicks ME, Jenson ML, Morris JE, Drasler WJ, Wilson GJ. 1997. Rheolytic thrombectomy with use of the AngioJet-F105 catheter: preclinical evaluation of safety. *J. Vasc. Interv. Radiol.* 8(6):939–45
 101. Siddiqi F, Blinc A, Braaten J, Francis CW. 1995. Ultrasound increases flow through fibrin gels. *Thromb. Haemost.* 73(3):495–98
 102. Siddiqi F, Odrlic TM, Fay PJ, Cox C, Francis CW. 1998. Binding of tissue-plasminogen activator to fibrin: effect of ultrasound. *Blood* 91(6):2019–25
 103. Smye SW, Berridge D, Ouriel K, Parkin A, David T. 1997. Assessing clot lysis strategies using a simplified mathematical model. *J. Med. Eng. Technol.* 21(3–4):121–25
 104. Steven FS. 1976. Polymeric collagen fibrils. An example of substrate-mediated steric obstruction of enzymic digestion. *Biochim. Biophys. Acta* 452(1):151–60
 105. Stewart UA, Bradley MS, Johnson CS Jr, Gabriel DA. 1988. Transport of probe molecules through fibrin gels as observed by means of holographic relaxation methods. *Biopolymers* 27(2):173–85
 106. Stringer HA, van Swieten P, Heijnen HF, Sixma JJ, Pannekoek H. 1994. Plasminogen activator inhibitor-1 released from activated platelets plays a key role in thrombolysis resistance. Studies with thrombi generated in the Chandler loop. *Arterioscler. Thromb.* 14(9):1452–58
 107. Tachibana K. 1992. Enhancement of fibrinolysis with ultrasound energy. *J. Vasc. Interv. Radiol.* 3(2):299–303
 108. Tebbe U, Tanswell P, Seifried E, Feuerer W, Scholz KH, Herrman KS. 1989. Single bolus injection of recombinant tissue-type plasminogen activator in acute myocardial infarction. *Am. J. Cardiol.* 64:448–53
 109. Tiefenbrunn AJ, Graor RA, Robison AK, Lucas FV, Hotchkiss A, Sobel BE. 1986. Pharmacodynamics of tissue plasminogen activator characterized by computer-assisted simulation. *Circulation* 73: 1291–99
 110. Topaz O, Vetrovec G. 1995. Laser for optical thrombolysis and facilitation of balloon angioplasty in acute myocardial infarction following failed pharmacologic thrombolysis. *Catheter Cardiovasc. Diagn.* 36(1):38–42
 111. Tuliani VV, O’Rear EA. 1997. Circulatory concentrations of fibrinolytic species during thrombolytic therapy estimated by stirred-tank reactor analysis. *Pharm. Res.* 14(8):1051–57
 112. Tyn MT, Guzek TW. 1990. Prediction of diffusion coefficients of proteins. *Bio-technol. Bioeng.* 35:327–38
 113. Uchida Y, Masuo M, Tomaru T, Kato A, Sugimoto T. 1986. Fiberoptic observation of thrombosis and thrombolysis in isolated human coronary arteries. *Am. Heart J.* 112:691–96
 114. Vaidya DS, Nitsche JM, Diamond SL, Kofke DA. 1997. Perturbation solution to the convection-diffusion equation with moving fronts. *AIChE J.* 43:631–44

115. Vakkalanka SK, Brazel CS, Peppas NA. 1996. Temperature- and pH-sensitive terpolymers for modulated delivery of streptokinase. *J. Biomater. Sci. Polym. Ed.* 8(2):119–29
116. Valji K, Bookstein JJ, Roberts AC, Davis GB. 1991. Pharmacomechanical thrombolysis and angioplasty in the management of clotted hemodialysis grafts: early and late clinical results. *Radiology* 178(1):243–47
117. Veklich Y, Francis CW, White J, Weisel JW. 1998. Structural studies of fibrinolysis by electron microscopy. *Blood* 92(12):4721–29
118. Virca GD, Travis J. 1984. Kinetics of association of human proteinases with human α_2 -macroglobulin. *J. Biol. Chem.* 259:8870–78
119. Voter WA, Lucaveche C, Erickson HP. 1986. Concentration of protein in fibrin fibers and fibrinogen polymers determined by refractive index matching. *Bio-polymers* 25:2375–84
120. Wagner HJ, Muller-Hulsbeck S, Pitton MB, Weiss W, Wess M. 1997. Rapid thrombectomy with a hydrodynamic catheter: results from a prospective, multicenter trial. *Radiology* 205(3):675–81
121. Walker J, Nesheim ME. 1994. Plasmin catalyzed degradation of noncrosslinked fibrin in a perfused clot. *Fibrinolysis* 8:111 (Abstr.)
122. Wall TC, Califf RM, George BS, Ellis SG, Samaha J, et al, for the TAMI-7 Study Group. 1992. Accelerated plasminogen activator dose regimens for coronary thrombolysis. *J. Am. Coll. Cardiol.* 19:482–89
123. Wang W, Boffa MB, Bajzar L, Walker JB, Nesheim ME. 1998. A study of the mechanism of inhibition of fibrinolysis by activated thrombin-activatable fibrinolysis inhibitor. *J. Biol. Chem.* 273(42):27176–81
124. Weiss HJ, Hawiger J, Ruggeri ZM, Turitto VT, Thiagarajan P, Hoffmann T. 1989. Fibrinogen-independent platelet adhesion and thrombus formation on subendothelium mediated by glycoprotein IIb-IIIa complex at high shear rate. *J. Clin. Invest.* 83(1):288–97
125. Weiss HJ, Turitto VT, Baumgartner HR. 1986. Role of shear rate and platelets in promoting fibrin formation on rabbit subendothelium. Studies utilizing patients with quantitative and qualitative platelet defects. *J. Clin. Invest.* 78(4):1072–82
126. Whitaker S. 1987. Mass transport and reaction in catalyst pellets. *Transp. Porous Media* 2:269–99
127. Williams S, Fatah K, Hjemdahl P, Blomback M. 1998. Better increase in fibrin gel porosity by low dose than intermediate dose acetylsalicylic acid. *Eur. Heart J.* 19(11):1666–72
128. Wiman B, Collen D. 1978. On the kinetics of the reaction between human antiplasmin and plasmin. *Eur. J. Biochem.* 84:573–78
129. Wu JH, Diamond SL. 1995. A fluorescence quench and dequench assay of fibrinogen polymerization, fibrinogenolysis, or fibrinolysis. *Anal. Biochem.* 224:83–91
130. Wu JH, Diamond SL. 1995. Tissue plasminogen activator (tPA) inhibits plasmin degradation of fibrin: a mechanism that slows tPA-mediated fibrinolysis but does not require α_2 -antiplasmin or leakage of intrinsic plasminogen. *J. Clin. Invest.* 95:2483–90
131. Wu JH, Siddiqui K, Diamond SL. 1994. Transport phenomena and clot dissolution therapy: an experimental investigation of diffusion-controlled and permeation-enhanced fibrinolysis. *Thromb. Haemost.* 72:105–12.
132. Yasukouchi T, Watanabe T. 1972. A new method based on one dimensional diffusion using small glass tubes for the measurement of fibrinolytic activity. *Thromb. Diath. Haemorrh.* 28(3):329–41
133. Zidansek A, Blinc A. 1991. The influence of transport parameters and enzyme

kinetics of the fibrinolytic system thrombolysis: mathematical modeling of two idealized cases. *Thromb. Haemost.* 65: 553–59

134. Zidansek A, Blinc A, Lahajnar G, Keber D, Blinc R. 1995. Finger-like lysing patterns of blood clots. *Biophys. J.* 69: 803–9



CONTENTS

A Dedication in Memoriam of Dr. Richard Skalak, <i>Thomas C. Skalak</i>	1
Tissue Engineering: Orthopaedic Applications, <i>C. T. Laurencin, A. M. A. Ambrosio, M. D. Borden, J. A. Cooper Jr.</i>	19
Airway Wall Mechanics, <i>Roger D. Kamm</i>	47
Biomechanics of Microcirculatory Blood Perfusion, <i>Geert W. Schmid-Schönbein</i>	73
Engineering and Material Considerations in Cell Transplantation, <i>Elliot L. Chaikof</i>	103
Bioreactors for Haematopoietic Cell Culture, <i>Lars Keld Nielsen</i>	129
Implanted Electrochemical Glucose Sensors for the Management of Diabetes, <i>Adam Heller</i>	153
Injectable Electronic Identification, Monitoring, and Stimulation Systems, <i>Philip R. Troyk</i>	177
Robotics for Surgical Applications, <i>Robert D. Howe, Yoky Matsuoka</i>	211
Transport of Molecules, Particles, and Cells in Solid Tumors, <i>Rakesh K. Jain</i>	241
Nucleic Acid Biotechnology, <i>Charles M. Roth, Martin L. Yarmush</i>	265
Fluid Mechanics of Vascular Systems, Diseases, and Thrombosis, <i>David M. Wootton, David N. Ku</i>	299
Automatic Implantable Cardioverter-Defibrillators, <i>William M. Smith, Raymond E. Ideker</i>	331
Engineering Aspects of Hyperthermia, <i>Robert B. Roemer</i>	347
3-D Visualization and Biomedical Applications, <i>Richard A. Robb</i>	377
Microfabrication in Biology and Medicine, <i>Joel Voldman, Martha L. Gray, Martin A. Schmidt</i>	401
Engineering Design of Optimal Strategies for Blood Clot Dissolution, <i>Scott L. Diamond</i>	427
Cellular Microtransport Processes: Intercellular, Intracellular and Aggregate Behavior, <i>Johannes M. Nitsche</i>	463
New Strategies for Protein Crystal Growth, <i>J. M. Wiencek</i>	505
Metabolic Engineering, <i>M. Koffas, C. Roberge, K. Lee, G. Stephanopoulos</i>	535
Ultrasound Processing and Computing: Review and Future Directions, <i>George York, Yongmin Kim</i>	559
Telemedicine, <i>Seong K. Mun, Jeanine W. Turner</i>	589
Imaging Transgenic Animals, <i>T. F. Budinger, D. A. Benaron, A. P. Koretsky</i>	611
Instrumentation for the Genome Project, <i>J. M. Jaklevic, H. R. Garner, G. A. Miller</i>	649